SYNTHESIS AND STRUCTURAL STUDIES OF CYCLIC BIOACTIVE CYSTEINE RICH PEPTIDES

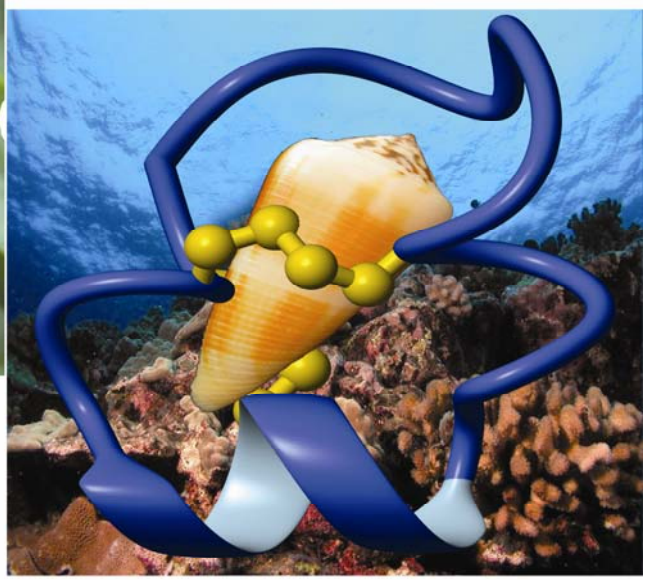

Lisbeth Sørum

Division of Chemical and Structural Biology
University of Queensland

Avdeling for legemiddelkjemi
Universitetet i Tromsø

May 2009

Abstract

Naturally occurring cyclic peptides have great therapeutic potential. Cyclotides are circular proteins found in the plants of the *Rubiaceae, Violaceae* and *Cucurbitaceae* families. They have an exceptional stability against chemical, enzymatic and thermal conditions due to their cyclic cystine knot (CCK) motif, which is the combination of a cyclic backbone and multiple disulfide bonds. In this thesis, kalata B5, a cyclotide from the bracelet subfamily, was synthesized and oxidized. The outcome was a misfolded product with different disulfide connectivity than the native kalata B5. The structure of this misfolded peptide was determined. It will potentially give useful information regarding factors that cause the misfolding of bracelet cyclotides. Members of the bracelet subfamily consist of up to 70% of the cyclotides. As these peptides have great potential as drug scaffolds, knowledge about the conditions that fold these cyclotides into their native fold will be essential.

Cyclotides display a wide range of bioactivities, but act as a host defense against insects and microorganisms in the plants that produce them. Two cyclotides from the subfamily Möbius, named kalata B1 and kalata B2, have already been investigated for their insecticidal activity. In this report the native cyclotide kalata B5 from the bracelet subfamily was investigated for its insecticidal activity.

Also presented in this thesis is the investigation of the cyclization of three analogues of conotoxin PVIIA. Conotoxins are tightly folded peptide toxins from the venom of cone snails. These peptides are small and disulfide rich and have shown to target ion channels and receptors with high specificity in the human brain and nervous system. These are important therapeutic targets and make the cyclotides very interesting as pharmacological tools, potential drugs or drug leads. However, as they are peptides they suffer from proteolytic degradation and have poor bioavailability. Cyclization of the backbone via a linker of amino acids would potentially increase their stability and hence their potential as therapeutics. A number of strategies were pursued to produce a cyclic analogue of PVIIA and a potentially successful approach was identified, but a cyclized PVIIA was not achieved yet. However, the cyclization of conotoxins has been successfully done with other conotoxins, therefore PVIIA has the potential to be cyclized. This will require some time to optimize the folding and cyclization conditions.

Acknowledgements

The work of my master thesis was performed at Institute of Molecular Bioscience, University of Queensland, Australia, in the period from October 2008 till May 2009.

First and foremost I wish to thank Dr Richard Clark for his guidance and support throughout the year. His encouragement with my project work and his many helpful comments on writing my thesis has been invaluable.

Special thanks go to Chia Chia Tan, Kathryn Greenwood and Angeline Chan for their much appreciated help in the lab with all the equipment, and Dr Norelle Daly for her very helpful work with structure calculations.

I would also like to thank Margaret Gentz and Cameron Tarbotton for their much appreciated help on writing my thesis and Bodil Carstens for her priceless support and motivating spirit throughout this year.

I would like to express my sincere gratitude to Prof. David Craik for providing the opportunity to work in his lab, and the whole Group Craik for making my stay here at IMB so enjoyable.

Finally, I would like to thank my supervisor at University of Tromsø, Norway, Jon Våbenø for giving me the permission to go to University of Queensland to do my master thesis.

Table of contents

List of Abbreviations

1D	One dimensional
2D	Two dimensional
Acm	Acetamidomethyl
Boc	*tert*-butoxycarbonyl
COSY	Correlated spectroscopy
cPVIIA	Cyclic PVIIA
CVO2	Cycloviolacin O2
CVO2nn	Cycloviolacin O2 non-native
Cys	Cysteine
DIPEA	*N,N*-Diisopropylethylamine
DMF	dimethylformamide
DMSO	Dimethylsulfoxide
DQF-COSY	Double quantum filtered correlated spectroscopy
ECOSY	Exclusive correlation spectroscopy
EDC	N-(3-Dimethylaminopropyl)-N-ethyl-carbodimide
ES-MS	Electrospray mass spectrometry
Fmoc	N-(9-fluoroenyl)methoxycarbonyl
Gly	Glycine

GSH	Reduced glutation
GSSG	Oxidized glutation
HBTU	2-(1H-Benzotriazole-1-yl)-1,1,3,3-tetramethyluronium hexafluorophosphate
HCl	Hydrochloride
HF	Hydrofluoric acid
kB5nn	Kalata B5 non-native
MeBzl	Methylbenzyl
MW	Microwave
NCL	Native chemical ligation
NEM	N-ethyl-maleimide
NMR	Nuclear magnetic resonance
NOE	Nuclear Overhauser effect
NOESY	Nuclear Overhauser effect spectroscopy
PAM	Phenylacetamidomethyl
PyBOP	Benzotriazol-1-yl-oxytripyrrolidinophosphonium
RMSD	Root mean square deviation
RP-HPLC	Reversed phase High Performance Liquid Chromatography
RTD-1	Rhesus theta defensin-1
SFTI-1	Sunflower trypsin inhibitor 1

SPPS	Solid Phase Peptide Synthesis
TCEP	Tris(2-carboxyethyl)phosphine
TFA	Trifluoroacetic acid
TOCSY	Total correlation spectroscopy

1 Introduction

1.1 Cyclic Cysteine Rich Peptides

Naturally occurring cyclic peptides have over the recent years been of great interest due to their increased stability over other peptides and wide range of bioactivities. These peptides have the unique feature that their N and C termini are joined together in an amide bond to form a cyclic backbone. Traditional peptides are amino acids in linear chains with open ends that are targets for proteolytic enzymes and, because of enzyme degradation and poor bioavailability, proteins have not been the favorites in the field of drug design so far. The recently discovered cyclic peptides show increased stability compared to their linear relatives, and are present in numerous species, ranging from plants and bacteria to mammals (1). Some examples are shown in Figure 1.

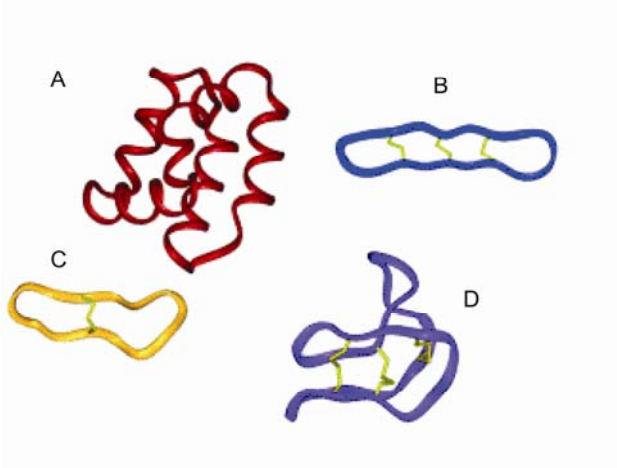

Figure 1: Four examples of circular proteins isolated from bacteria, plants and mammals. A: bacteriocin AS-48 from E. faecalis*. B: RTD-1 from the leukocytes of macaques. C: SFTI-1 from sunflower seeds. D: the cyclotide kalata B1 from* O. affinis*. Disulfides bonds are shown in yellow in B, C and D (1).*

The discovery of these peptides started in the mid 1990s when circular proteins from plants, now known as the cyclotides, were discovered in plants. Their real discovery was actually in the early 1970s when a tea extract from the plant *Oldenlandia affinis* was reported to give uteronic activities, but the actual structure was not determined until almost thirty years later

(2). Since then several other circular peptides have been isolated too; bacteriocin AS-48 isolated from *Enterococcus faecalis* is the largest circular peptide so far with 70 amino acids (3). Other examples are *Rhesus* theta defensin-1 (RTD-1), a new type of defensin (small disulfide-rich peptides involved in host defense) from mammals (4), or the circular peptide sunflower trypsin inhibitor 1 (SFTI-1), which is found in the seeds of sunflowers (5). These examples are summarized in Figure 1. The bonds shown in yellow in the figure are disulfide bonds formed between multiple cysteines in the backbone, which contributes to stability by serving as a defense mechanism for the proteins against the extracellular environment (6). SFTI-1 and kalata B1 (Figure 1 C and D) are examples of peptides with a high content of well conserved cysteines that form cross linking disulfide bonds. These multiple disulfide bonds facilitate the formation of a well-defined and conformational stable three dimensional structure by the peptides (6). A cyclized backbone together with multiple disulfide bonds gives the peptide an exceptional stability against protease digestion and thermal denaturation. Many cysteine rich peptides display specific biological activities and have been of interest in the field of pharmacology and drug design, but have been commercially limited due to disadvantages with proteolytic degradation *in vivo*. The discovery of increasing numbers of naturally cyclic peptides has given ideas to develop synthetic techniques to make naturally linear peptides cyclic. This approach has the potential to improve their bioavailability and thus their potential as drug leads. Peptides whose termini are in reasonable close proximity to each other have the potential to be cyclized and still maintain their structure and hence bioactivity (7-9).

This project will focus on two classes of disulfide rich peptides; the conotoxins and the cyclotides. I have investigated the synthesis and cyclization of the linear conotoxin PVIIA, a peptide that targets the voltage-gated potassium channel in the nervous system. Linear peptides, like the conotoxins, suffer from disadvantages with *in vivo* degradation, so a cyclic backbone will increase their bioavailability. Its structure will be determined and the bioactivity assessed.

The other part of my thesis concerned the cyclotide kalata B5, which I have synthesized and oxidized in this thesis. Its structure was also determined and investigated. The cyclotides are known for their extremely structural stability, and in addition to their range of bioactivities and sequence diversities, these peptide ligands are invaluable as pharmacological tools and as

platforms for developing therapeutic and agricultural agents. An aim is therefore to find efficient methods to synthesize and fold kalata B5 into its native conformation.

Kalata B1 and kalata B2, two other cyclotides, have shown to display insecticidal activity, and due to previous reports that kalata B5 is a more potent insecticidal its activity will be assayed in this project.

1.2 Cyclotides

1.2.1 The Discovery of the Cyclotides

The cyclotides are a unique family of naturally occurring cyclic peptides from plants of the *Rubiaceae, Violaceae* and *Cucurbitaceae* families. They are 28-37 amino acids in size with three disulfide bonds and are characterized by a cyclized backbone with an interlocking arrangement of the disulfide bonds.

The cyclotide kalata B1 was first discovered as a uterus-contractive when an extract from the plant *Oldenlandia affinis* was used as a tea by African women to accelerate childbirth. It says a lot about the extreme stability of the peptide that after boiling the plant material the bioactivity was still maintained very well (10). The ability to be taken orally is also rare in peptide drugs. The extreme stability *in vivo* makes the cyclotides very attractive as potential agricultural and pharmaceutical applications (11, 12). Around 100 cyclotides have so far been isolated from the *Rubiaceae, Violaceae* and *Cucurbitaceae* families (13).

1.2.2 The Cyclotide Structure

The cyclotides have an amide head-to-tail cyclized backbone which means that their N and C termini are linked together via a peptide bond. Their six highly conserved cysteines make a knotted arrangement of three disulfide bonds. An embedded ring is formed by two disulfide bonds and their connecting backbone segments and the third disulfide bond penetrates this ring. The combination of a cystine knot embedded in a cyclic backbone is known as the cyclic

cystine knot motif (CCK) and it gives a unique protein fold that is topologically complex and has exceptional stability against chemical, enzymatic and thermal conditions (12).

The various segments of the backbone between the six conserved cystine residues are called loops. Some of these loops are highly conserved, like loop 1 and 4 which form the core of the cystine knot, while the other has a high degree of variability (12, 14). The three dimensional structures determined to date show that the disulfide bonds are occupying the interiors of the cyclotides which make the hydrophobic residues expose at the surface of the protein (13). This is opposite to conventional proteins which have their hydrophilic residues on the surface.

Due to their sequences the cyclotides were originally sorted into two subfamilies; the Möbius and bracelet (Figure 2). This is based on the presence or absence of a cis-proline in loop 5, which the Möbius group has and the bracelet lacks (15). After the discovery of MCoTI-I and MCoTI-II, two trypsin inhibitors from the seeds of the plant *Momordica cochinchinensis* of the *Cucurbitaceae* family, the cyclotides expanded to three subfamilies (16). Figure 3 shows some representative sequences from all three subfamilies.

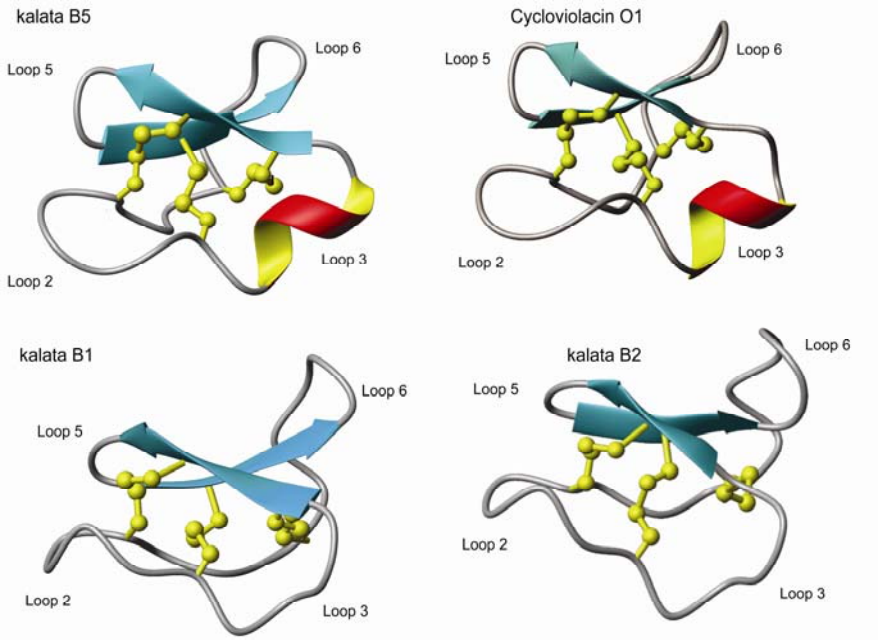

Figure 2: Three dimensional structures of different cyclotides. Kalata B1and kalata B2 are examples of cyclotides from the subfamily Möbius, whereas kalata B5 and cycloviolacin O1 are examples from the bracelet subfamily. Typical for the bracelet subfamily is to have an α-helix in loop 3 as shown here.

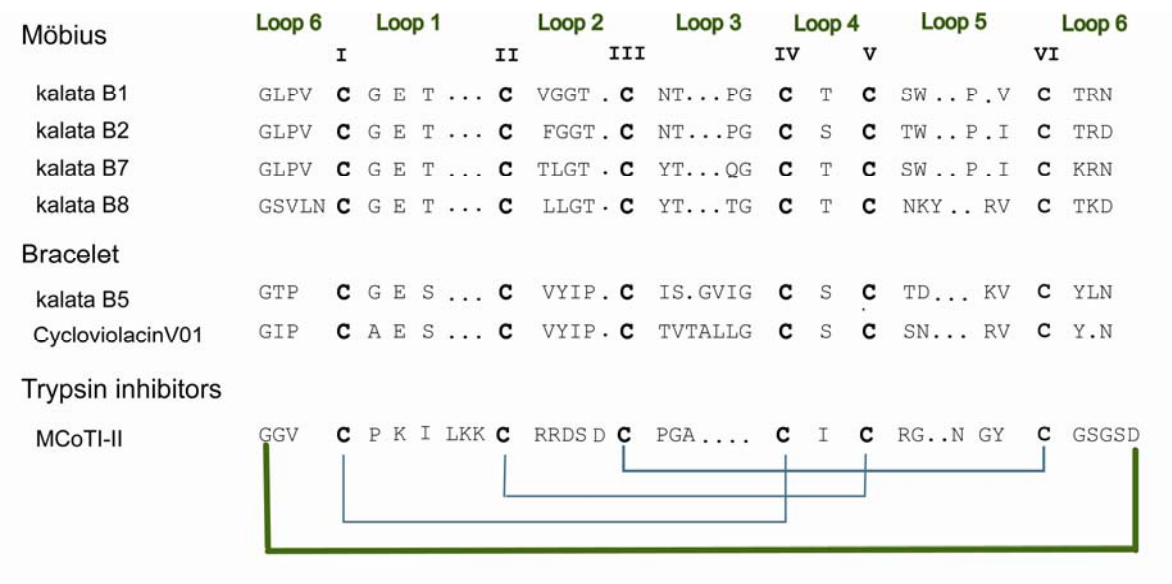

Figure 3: Sequence alignments of some examples of cyclotides from the subfamilies Möbius, bracelet and trypsin inhibitors, showing their disulfide connectivities in blue. The cysteine residues are numbered with Roman numbers, and the backbone loops between the cysteine residues with green letters. The cyclic backbone is shown as the thick green line.

Kalata B8 has sequence similarities with both the Möbius and bracelet subfamilies and hence can be considered to be a hybrid of the two subfamilies. Loop 2 and loop 3 match the corresponding loops in kalata B1 and B2, whereas loop 5 resembles the bracelet cyclotides. Kalata B8 has also shown to be the most hydrophilic of all cyclotides isolated from *O. affinis* (17).

1.2.3 Cyclotide Activity and Therapeutic Applications of Cyclotides

There are several reports of the varied biological activities of cyclotides. In addition to their activity on the uterus, they also have antimicrobial (18), hemolytic (19), anti-HIV (20), neurotensin antagonism (21), cytotoxic (18), antitumor (22) and antifouling activities (23). However, their natural function seems to be as a host defense against microorganisms and insects. In particular kalata B1 and kalata B2 have been shown to inhibit the growth and development of *Helicoverpa armigera* and *H. punctigera* (11), which are the main insect pests for important crop plants like cotton and are therefore of major importance regarding

pest management. Because the cyclotides are gene products and act as natural insecticides in their host plants, they could be a potential new group of crop protection agents. By introducing the cyclotide gene into cotton plants they would perform their insecticidal activities there. Today more than 80% of the cotton plants are transgenic (24) and together with integrated pest management (IPM) this has given a 60% reduction in pesticide use over the last ten years (25). IPM for cotton is a system that integrates all means of managing pest populations with the aim of reducing insecticide use while maintaining profitability, yield, fibre quality and crop maturity. A reduction in pesticide use is also beneficial for the biodiversity in and around the cotton field. Until the introduction of genetically modified plants that could produce their own toxins the main pests were controlled by synthetic insecticides, which is more harmful to the environment (24, 25).

It is believed that the cyclotide plants produce a suite of cyclotides to protect themselves against a range of insect pests. For example there are about 20 cyclotides present in *O. affinis* (14). Kalata B1 and kalata B2, the two most studied cyclotides, differ by only five conservative substitutions and both of them show insecticidal activity. There is now interest to examine other cyclotides with more diverse structural characteristics.

1.2.4 Kalata B5

Kalata B5 is one of the cyclotides isolated from *O. affinis* (14), but its expression varies with the seasons (unpublished data, M. Plan). It belongs to the bracelet subfamily and preliminary reports suggested that this cyclotide was approximately 10-fold more active as an insecticidal than kalata B1 (unpublished data, M. Plan). Kalata B5 has significant differences in its sequence (Figure 3 and Figure 4) compared to kalata B1 and B2 and is for that reason of interest concerning insecticidal activity. Figure 5 shows the three dimensional structure of kalata B5. The aim of this study was to develop synthetic strategies to produce kalata B5 and to confirm its insecticidal activity.

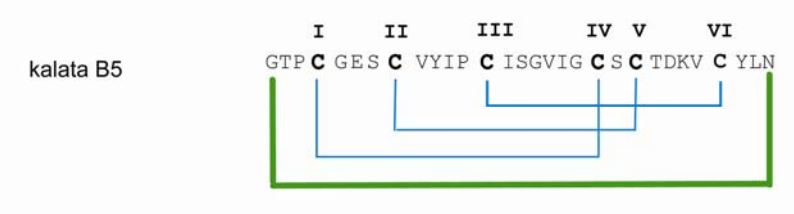

Figure 4: The sequence of kalata B5 with its disulfide connectivities (blue lines), loops and cyclic backbone (green thick line).

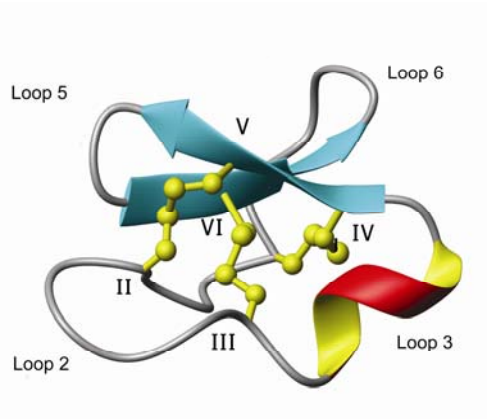

Figure 5: A three dimensional representation of the structure of kalata B5 showing the CCK motif, which is composed of the cyclized peptide backbone and a knotted disulfide topology. The β-sheets are in an anti parallel formation and indicated by the big blue arrows. A characteristic feature of the bracelet cyclotides is an α-helix in loop 3, here shown as the red and yellow coil. The six cysteines are labeled with Roman numerals and show the disulfide connectivity; I-IV, II-V, III-VI.

1.3 Conotoxins

1.3.1 The *Conus* Genus

Conotoxins are relatively small disulfide rich peptide toxins found in the venom of cone snails, a large group of carnivorous marine snails that belongs to the genus *Conus*. The venom is the main weapon these carnivorous predators use to capture prey, but it is also believed that the venom is used for defense and competition. These cone snails hunt fish, mollusks and worms and inject their venom through a hollow harpoon-like tooth, which, because of several neurotoxins, causes rapid immobilization of the prey (26, 27). The genus consists of more than 500 species found in tropical marine habitats where each of these species contains probably more than 100 different peptides, giving an estimate of > 50.000 different components present in venoms of all living cone snails (Terlau and Olivera 2004). Today, less than 0.1% of these compounds have been characterized pharmacologically (28) and those already characterized have shown to be highly selective for a wide range of ion channels and receptors in the brain and nervous system of humans (26). With a natural library of more than 50.000 bioactive peptide toxins, a rich source of potential new therapeutics or drug leads is waiting to be explored.

The conotoxins are in the range of 10-30 residues and consist of tightly folded structures with up to five disulfide bonds that provide the conotoxins with high stability compared with non-disulfide-bonded peptides (Figure 6). The majority of the conotoxins characterized contain only two or three disulfide bonds (26, 29). The conotoxins are unusual in their high content of post-transcriptional modifications, including amidation, glycosylation, and epimerization, and they often contain unusual amino acids, such as hydroxyproline and γ–carboxyglutamic acid. These post-transcriptional modifications enhances the molecular diversity of this peptide class even more (30), but can complicate their chemical synthesis and characterization.

```
A  GIIIB      . ....RD  C  C  TOORK  C  KDRR  C  KPMKC  C  A
B  MII       . .....G  C  C  SNP.V  C  HLEH  S  ...NL  C  .
C  MVIIA   C  KGKGAK  C  S  RLMYD  C  CTGS  C  .RSGK  C  .
D  PVIIA  C  RIONQK  C  F  QHLDD  C  CSRK  C  NRFNK  C  V
```

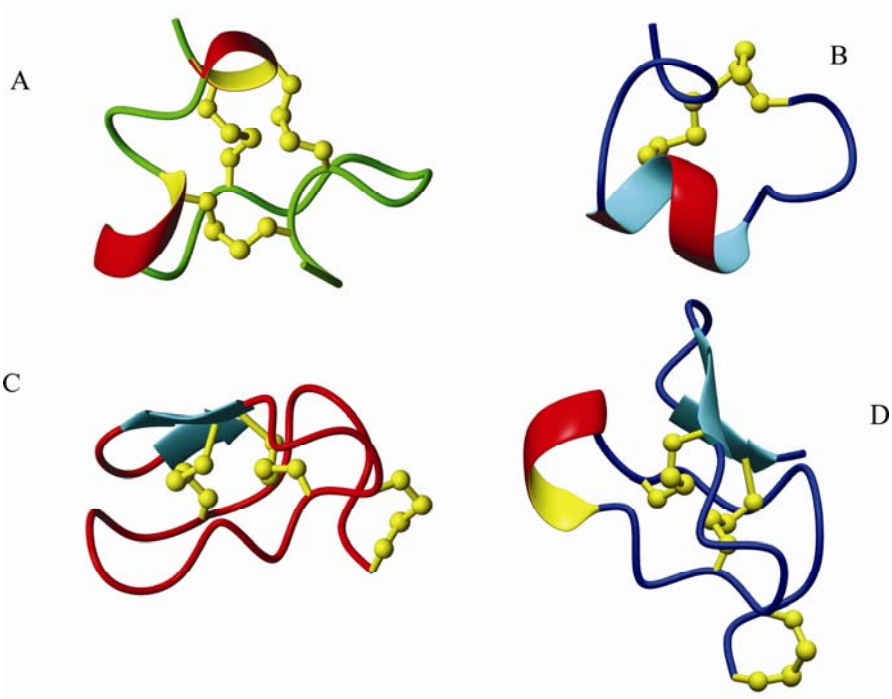

Figure 6: Image of the structures of several conotoxins representative of different classes. The structures here are: A: μ-conotoxin GIIIB from C. geographus*, B: α-conotoxin MII from* C. magus*. C: ω–conotoxin MVIIA from* C. magus*. D: κ-conotoxin PVIIA from* C. purpurascens*. The β–strands are shown as arrows, the α-helixes are in red and yellow, and the disulfide bonds are shown in yellow ball-and-stick format (31). Their corresponding sequences are shown below with cysteines shown in bold. O = hydroxyproline.*

Based on the cysteine framework and the pharmacological activity, the wide range of different conotoxins has been divided into major classes. Table 1 shows amino acid sequences with cysteines (yellow) aligned within each structural framework, and the disulfide connectivity for each of the classes are shown in Figure 7 (29). Individual peptides are named with a Greek letter to indicate the pharmacological activity, one or two letters to indicate the *Conus* species from which the peptide was first isolated, a Roman numeral to indicate the disulfide framework category, and an upper-case letter to denote the order of discovery within that category (31).

Table 1

Five Major Classes of Conotoxins and their Disulfide Connectivity

Table 1: The six major classed of conotoxins and their disulfide connectivity																																				
α-conotoxins (2 loop framework peptides that inhibit nicotinic acetylcholine receptors)																																				
GI			E	**C**	**C**	N	-	P	A	**C**	G	R	H	Y	S	-	-	**C***																		
SIA			Y	**C**	**C**	H	-	P	A	**C**	G	K	N	F	D	-	-	**C***																		
MII			G	**C**	**C**	S	N	P	V	**C**	H	L	E	H	S	N	L	**C***																		
PnIA			G	**C**	**C**	S	L	P	P	**C**	A	A	N	N	P	D	Y	**C***																		
μ-conotoxins (3 loop framework that block sodium channels)																																				
GIIB		R	D	**C**	**C**	T	O	O	R	K	**C**	K	D	R	R	**C**	K	O	M	K	**C**	**C**	A*													
GIIC		R	D	**C**	**C**	T	O	O	K	K	**C**	K	D	R	R	**C**	K	O	L	K	**C**	**C**	A*													
ω-conotoxins (4 loop framework peptides that block calcium channels)																																				
GVIA		**C**	K	S	O	G	S	S	**C**	S	O	T	S	Y	N	**C**	**C**	-	R	S	**C**	N	O	Y	T	K	R	**C**	Y						
SVIA		**C**	R	S	S	G	S	O	**C**	G	V	T	S	I	-	**C**	**C**	G	R	-	**C**	-	-	Y	R	G	K	**C**	T*						
MVIIA		**C**	K	G	K	G	A	K	**C**	S	R	L	M	Y	D	**C**	**C**	T	G	S	**C**	R	S	-	-	G	K	**C***							
δ-conotxins (4 loop framework peptides that delay inactivation of sodium channels)																																				
TxVIA			W	**C**	K	Q	S	G	E	M	**C**	N	L	L	D	Q	N	**C**	**C**	D	G	Y	-	**C**	I	V	L	V	**C**	T					
GmVIA	V	K	P	**C**	R	K	E	G	Q	L	**C**	D	P	I	F	Q	N	**C**	**C**	R	G	W	N	**C**	-	V	L	F	**C**	T					
PVIA		E	A	**C**	Y	A	P	G	T	F	**C**	G	I	K	O	G	L	**C**	**C**	S	E	F	-	**C**	L	P	G	V	**C**	F	G*				
κ-conotoxins (4 loop framework peptide that blocks Shaker potassium channel)																																				
PVIIA			**C**	R	I	O	N	Q	K	C	F	Q	H	L	D	D	**C**	**C**	S	R	K	**C**	N	R	F	N	K	**C**	V						

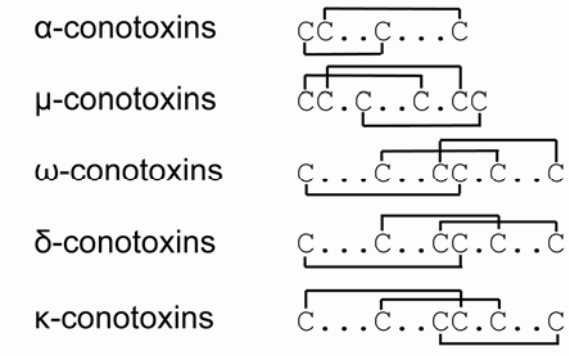

Figure 7: The five major classes of conotoxins and their disulfide connectivity (29)

It is believed that the specific sequence of each peptide accounts for the specificity for various voltage-gated channels and receptors in the brain and nervous system. For example PVIIA, which is a κ-conotoxin (Table 1), is specific for potassium voltage-gated channels whereas α- and ω-conotoxins are specific for the acetylcholine receptors and calcium channels, respectively. The sodium channels are targeted by both the μ- and δ-conotoxins but have different actions. The μ-conotoxins block the sodium channel, whereas the δ-conotoxins delay their inactivation. (27, 31). The neuronal receptors and ion channels targeted by these conotoxins (32) control a diverse range of biological processes and are therefore important

therapeutic targets (33). Therefore, the conotoxins are valuable pharmacological tools and potential drug leads, or drug themselves, against a variety of neurological disorders (34, 35).

1.3.2 Therapeutic Applications of Conotoxins

Conotoxins target membrane-bound protein channels and receptors and show exquisite specificity and potency for important physiological targets. They are among the smallest bioactive peptides and hence relatively easy to synthesize, and their post-transcriptional modifications and multiple disulfide bonds improve their structural stability. Because of these unique features the conotoxins can provide leads for potential new therapies (28, 31). For example the ω-conotoxin MVIIA acts as an analgesic by blocking the N-type voltage-dependent calcium channels, and a synthetic version ziconotide (Prialt®) is now used as an analgesic drug (36) for the treatment of severe chronic pain in people who cannot use standard pain-relieving medications. Ziconotide has been shown to have additive value to the effect of morphine, but does not have the addictive properties (37).

On the basis of their hydrophilic properties and relatively large size compared to other oral drugs, conotoxins have limitations when it comes to oral administration. Because the peptides are generally not able to cross epithelial layers they suffer from poor oral bioavailability. The drawback of Prialt® is also its administration as it has to be administered via direct spinal infusion. The oral route of administration is generally preferred for conventional pharmaceuticals instead of administration routes like intravenous, intramuscular, or epidural injection. The challenge in the future will be to optimize the peptide delivery *in vivo*, which is a big step in the direction of determining whether these peptides can be candidates for drug development or not (28).

1.3.3 Limitations of conotoxins and how to overcome them

Like most peptides, conotoxins suffer from disadvantages of poor stability and short biological half-lives *in vivo* because of proteolytic degradation in human plasma (8, 31). Due to the presence of the disulfide bonds they are possibly less effected compared to non-

disulfide peptides, but it is believed that there is a significant value in stabilizing conotoxins for improving their absorption and delivery and half lives *in vivo* (31).

Exopeptidases are a particular class of proteases in the body that attack the free N and C termini of peptides by cleaving amino acids from the end of the molecule. But if the two ends are joined together the molecule is protected from these proteases because the N and C termini will disappear. The structure of the protein will also be stabilized when it is cyclized because the conformational energy of the unfolded state is decreased (38) and this will give the molecule rigidity (39). Cyclization is already widely used in the pharmaceutical industry as a technique to stabilize the conformation of short non-disulfide bonded peptides.

The cyclotide family, which is naturally cyclic disulfide-rich peptides from plants, has chemical and physical properties that overcome the limiting properties of normal peptides when it comes to chemical denaturation and enzymatic degradation *in vivo*. This is because of their unique cyclic backbone and knotted arrangement of disulfide bonds (see chapter 1.2.2). If the conotoxins could aquire this stability and bioavailability their potential to be used therapeutically would increase dramatically. This has been done for the α-conotoxin MII by using linkers of six or seven amino acids to cyclize its peptide backbone (Figure 8). The engineered peptide kept its full activity but has improved its resistance to enzymatic degradation (8). This has also been successfully done to the χ-conotoxin MrIA which has been backbone-cyclized by a two amino acid linker. Resistance to proteolysis was improved while the activity was maintained (9). Therefore, backbone cyclization of peptide toxins has the potential to protect these molecules form degradation and improve their oral bioavailability.

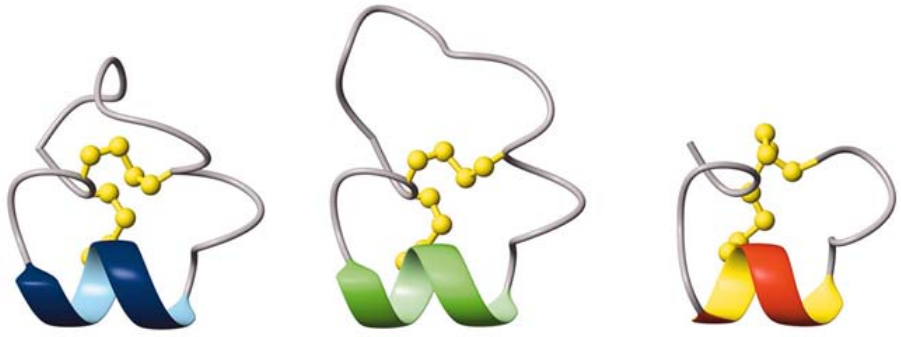

Figure 8: Cyclization of the linear conotoxin MII by use of six- or seven residue linkers to join the C- and N-termini of the peptide (8). The three dimensional structures of cMII-6 (left) and cMII-7 (middle) and the native MII (right).

In this project I intend to synthesize three cyclic analogues of the κ -conotoxin PVIIA and characterize their structure and biological activity.

1.3.4 PVIIA

The κ-conotoxin PVIIA is a 27-residue peptide from the venom of the purple cone snail *C. purpurascens.* Figure 9 shows its three dimensional structure and sequence, where O represents 4-*trans*-hydroxyproline (27).

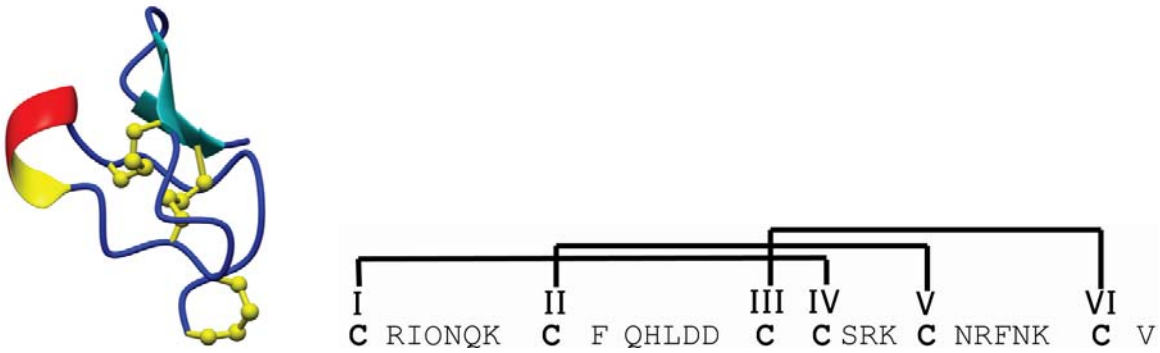

Figure 9: Three dimensional structure of PVIIA. The β–strands are shown as blue arrows and the α-helix in red and yellow. The disulfide bonds are shown in the yellow ball-and-stick format (31). The sequence of PVIIA is shown to the right with its cysteines in bold and disulfide connectivity shown by the black lines. O = hydroxyproline.

The peptide has three disulfide bonds arranged in a knotted topology (I-IV, II-V, III-VI) (40) and four loops, and has been shown to block the *Shaker* potassium channel by binding in a voltage-sensitive manner to the external vestibule of the channel and physically occlude the pore (33). Because PVIIA acts rapidly on the potassium voltage-gated channel it is believed that this peptide has an important role in the fast excitotoxic immobilization of the prey after the venomous sting (27). The sequence of κ-PVIIA is very different from the sequences of other toxins, like dendrotoxins or scorpion and spider toxins, which are peptides that also block the *Shaker* potassium channels (40). PVIIA can be very valuable as a probe of potassium channel structure or as a ion channel therapeutic. The peptide has the unique ability

to discriminate between the types of ion channels which are not achieved by the small molecule drugs that dominate the pharmaceutical industry today (29).

The aim of this study is to design and synthesize three cyclic PVIIA analogues by joining the N- and C-termini of the backbone via a linker of different lengths (TRNG, GGAAGG, and GGAAGAG) as shown in Figure 10.

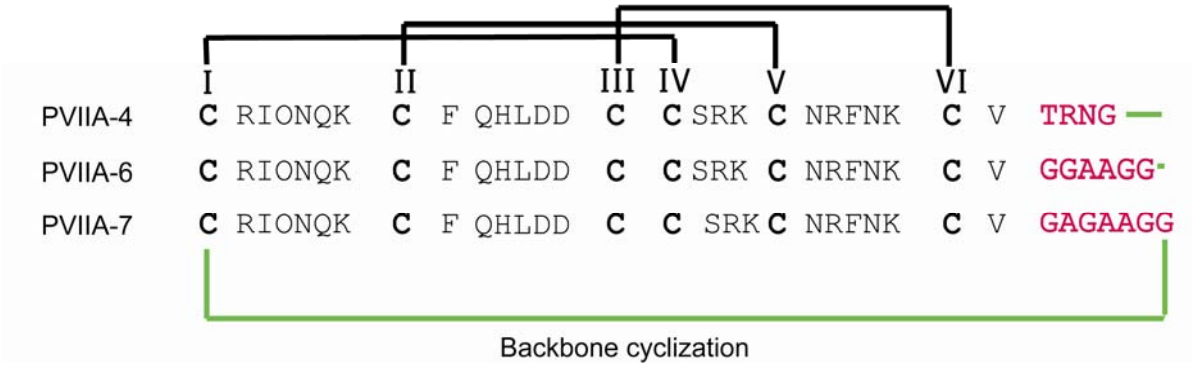

Figure 10: The three analogues of PVIIA with their different linker sizes shown in pink letters. The green line indicates between which amino acids in the sequence the cyclic backbone will form. O = hydroxyproline.

The amino acids in the first linker, TRNG, are from the corresponding loop in the cyclotide kalata B1 whereas Gly and Ala residues were used in the second two linkers due to their small side chains and hence a reduced likelihood of the linker interacting with the rest of the molecule. It has previously been demonstrated that the length of the linker used to span the distance between the termini is a crucial factor in maintaining a biological active peptide (8). The structure of the cyclic version of PVIIA (referred as cPVIIA) will then be determined and the new stability and activity will be assessed.

1.4 Aims

- Synthesize and characterize the bracelet cyclotide kalata B5 and test its activity against *H. armigera*.
- Synthesize three cyclic analogues of κ-conotoxin PVIIA, determine their structure and test their stability doing stability assays.

1.5 Design and synthesis of disulfide rich peptides

1.5.1 Solid-Phase Peptide Synthesis (SPPS)

Since its implementation in the 1960s, Solid Phase Peptide Synthesis (SPPS) has become the standard methodology for the synthesis of small peptides. The concept is to grow a peptide chain on to a solid support consisting of resin beads. When the growing peptide chain is built on this solid support, reaction reagents and byproducts of the synthesis can be readily flushed away while the peptide attached to the resin is retained (41). The amino acids are built in a C to N terminal direction, which is backwards to how the sequence is written. The general principle is based on a coupling-deprotection cycle which is repeated until the last amino acid is attached. After deprotection of the amino acid the free N terminus amine of the peptide is coupled to a single N-protected amino acid, which is then deprotected revealing a new N terminus amino before another amino acid is added (Figure 11). There are two types of chemistry used in SPPS; Boc and Fmoc. Both are described below (42).

1.5.2 Boc- and Fmoc-Chemistry

SPPS using *tert*-butoxycarbonyl (Boc) chemistry is a methology where acid labile protecting groups are used. To remove the Boc group from the growing peptide acidic conditions is necessary and trifluoroacetic acid (TFA) is usually used. N-(9-fluoroenyl)methoxycarbonyl (Fmoc) chemistry is the other method in SPPS which utilizes base (piperidine; 20% piperidine in DMF) for the deprotection step. In Boc-chemistry removal of the peptide from the resin and the side-chain protecting groups at the end of the synthesis is attained by incubating in hydrofluoric acid (HF), a reaction that can be dangerous, whereas in Fmoc-chemistry cleavage and deprotection of the peptide is performed by treating the resin with TFA, which is easier and safer (42).

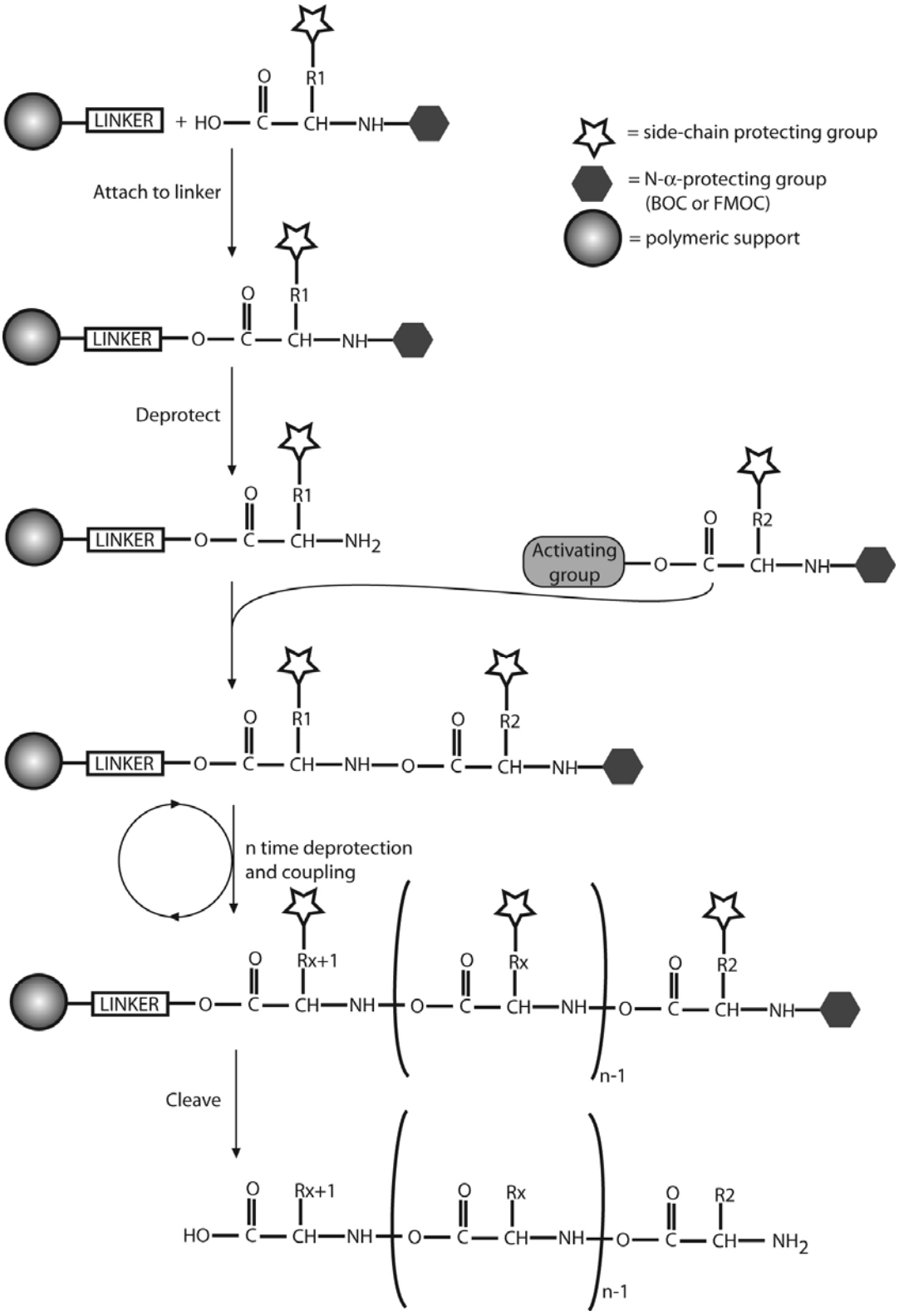

Figure 11: The general principle of SPPS using either Boc or Fmoc chemistry.

1.5.3 Native chemical ligation

Native chemical ligation (NCL) is a method for constructing a large polypeptide from two unprotected peptides (43). This strategy requires the use of a thioester linker between the resin and the C-terminus of the peptide. The general principle of NCL is a chemoselective reaction between a peptide containing a C-terminal thioester with a peptide with an N-terminal cysteine. This reaction will proceed in the presence of a thiol catalyst and the C-terminal thioester undergoes nucleophilic attack by the side chain of the cysteine residue at the N-terminal of the other peptide. The initial thioester-linked intermediate rearranges spontaneous in the same reaction conditions to form the favorable geometric arrangement which is the native peptide bond at the ligation site. The principles of NCL can be used to produce cyclic peptides as demonstrating in Figure 12. By synthesizing a peptide with an N terminus cysteine and a thioester on the C terminus an intramolecular NCL reaction during the HF cleaving will form an amide binding between the N and C termini and hence make the backbone of the peptide cyclic. This technique will be used in this project to cyclize small peptides. NCL is limited to reaction at an N-terminal cysteine residue because of the SH-containing side chain. The thioester linker is base labile and incompatible with the Fmoc deprotection step, thus disfavoring Fmoc chemistry (43). Hence Boc chemistry has to be used whenever cyclic peptides are synthesized.

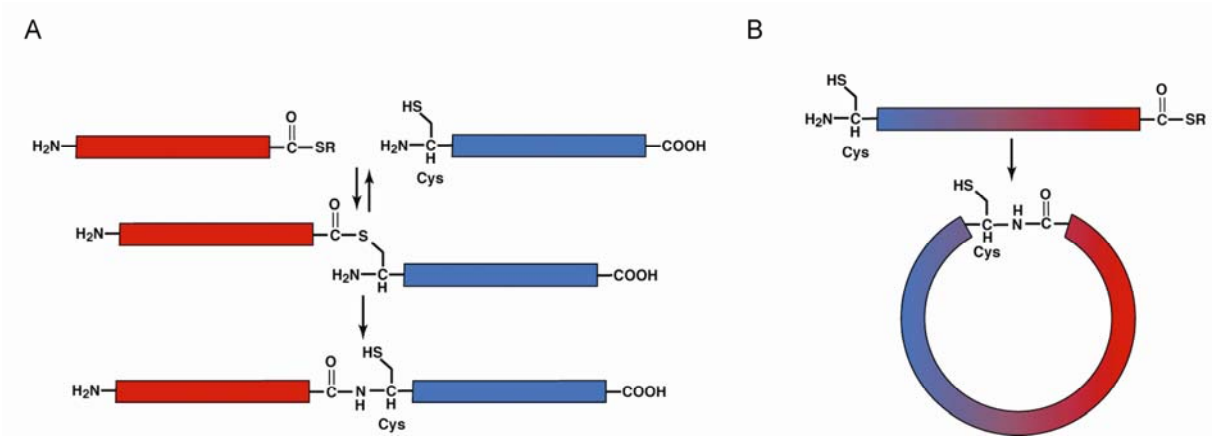

Figure 12: A: The principle of native chemical ligation. The product contains a native peptide bond. B: the principles of NCL used to produce cyclic peptides.

1.5.4 Protein folding and cyclization

Oxidation of peptides forms the disulfide bridges between the cysteines and folds the peptides into their correct three dimensional structures. In a peptide with more than two cysteines an oxidation can produce a number of non native disulfide isomers in addition to the native one. As there are a large number of possible disulfide isomers that can be produced (15 for six cysteines) it is often difficult to determine the optimum oxidative folding conditions required to form the desired disulfide isomer *in vitro* and a range of conditions have to be examined. Disulfide-rich peptides like the conotoxins and cyclotides are of great interest when it comes to oxidative folding mechanisms. As described earlier the disulfide bonds in the cyclotides form a CCK. Given the topological complexity of the CCK, intermediates present in the oxidative folding pathway would be of interest to understand the formation of the CCK. Knowledge about the intermediates or misfolded products could potentially lead to assistance in the design and optimization of the synthesis of engineered cyclotide and conotoxin analogs. (44).

2 Results

2.1 Cyclotides

2.1.1 Peptide Synthesis and Oxidative Folding of Kalata B5

Kalata B5 was manually synthesized using Boc chemistry SPPS with an average coupling yield per amino acid of 99.3%. To make the backbone cyclic the NCL strategy (chapter 1.5.3) was used. Since the NCL requires a cysteine residue at the N terminus, Gly19 was chosen as the start point and Cys20 the endpoint for the synthesis. The sequence is shown in the introduction (chapter 1.2.4). After the last amino acid was coupled the peptide was cleaved from the resin with HF/*p*-cresol/*p*-thiocresol (18:1:1 *v*/*v*/*v*) at -5-0˚C for 1.5 hour. The residual HF was evaporated, and the crude peptide was washed with cold diethyl ether, filtered and redissolved in 50% acetonitrile containing 0.1% TFA and lyophilized. After identification and purification of the linear peptide by ES-MS and RP-HPLC (Figure 13 and Figure 14), the fully reduced peptide was oxidized in 0.1 M NH_4HCO_3 and propan-2-ol (50:50 *v*/*v*) (condition 18, Appendix 1) to yield a mixture of disulfide isomers.

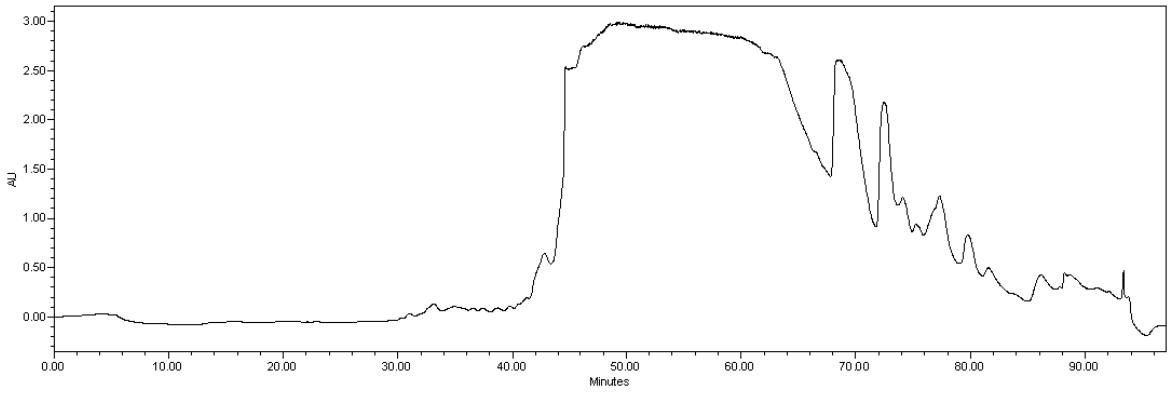

Figure 13: HPLC trace of crude kalata B5. The peptide elutes after approximately 45 minutes.

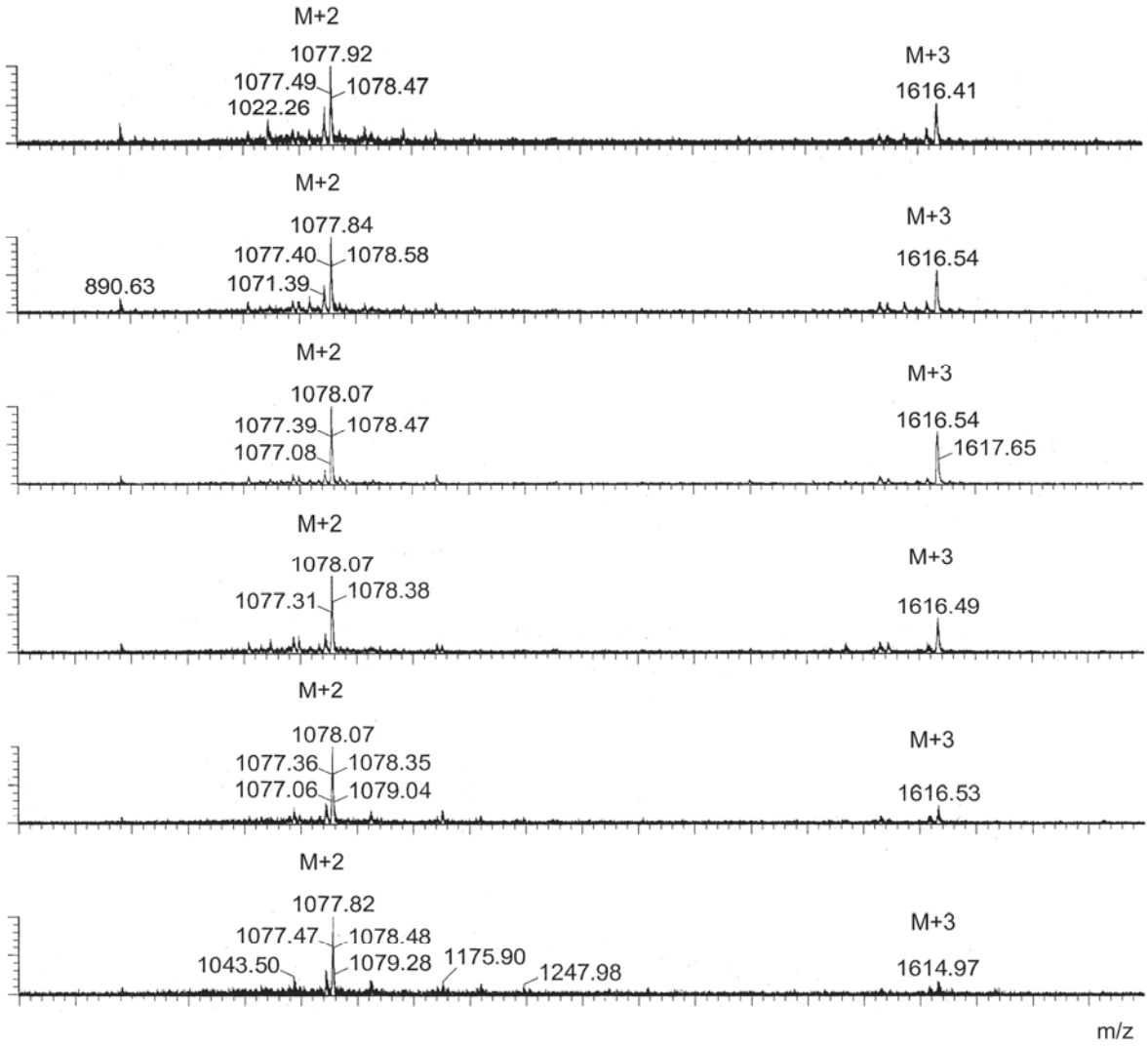

Figure 14: ES-MS of the collected fractions. M+2 and M+3 of fully reduced kalata B5 are shown in the spectrum. Calculated MW for the linear peptide with the thioester included is 3230.6 g/mol.

A series of different oxidation conditions were examined and Figure 15 show six examples of in total 13 different oxidation conditions that were examined for kalata B5 (condition 3, 9, 18, 21, 22, 24-26, 28 and 31-34 in Appendix 1).

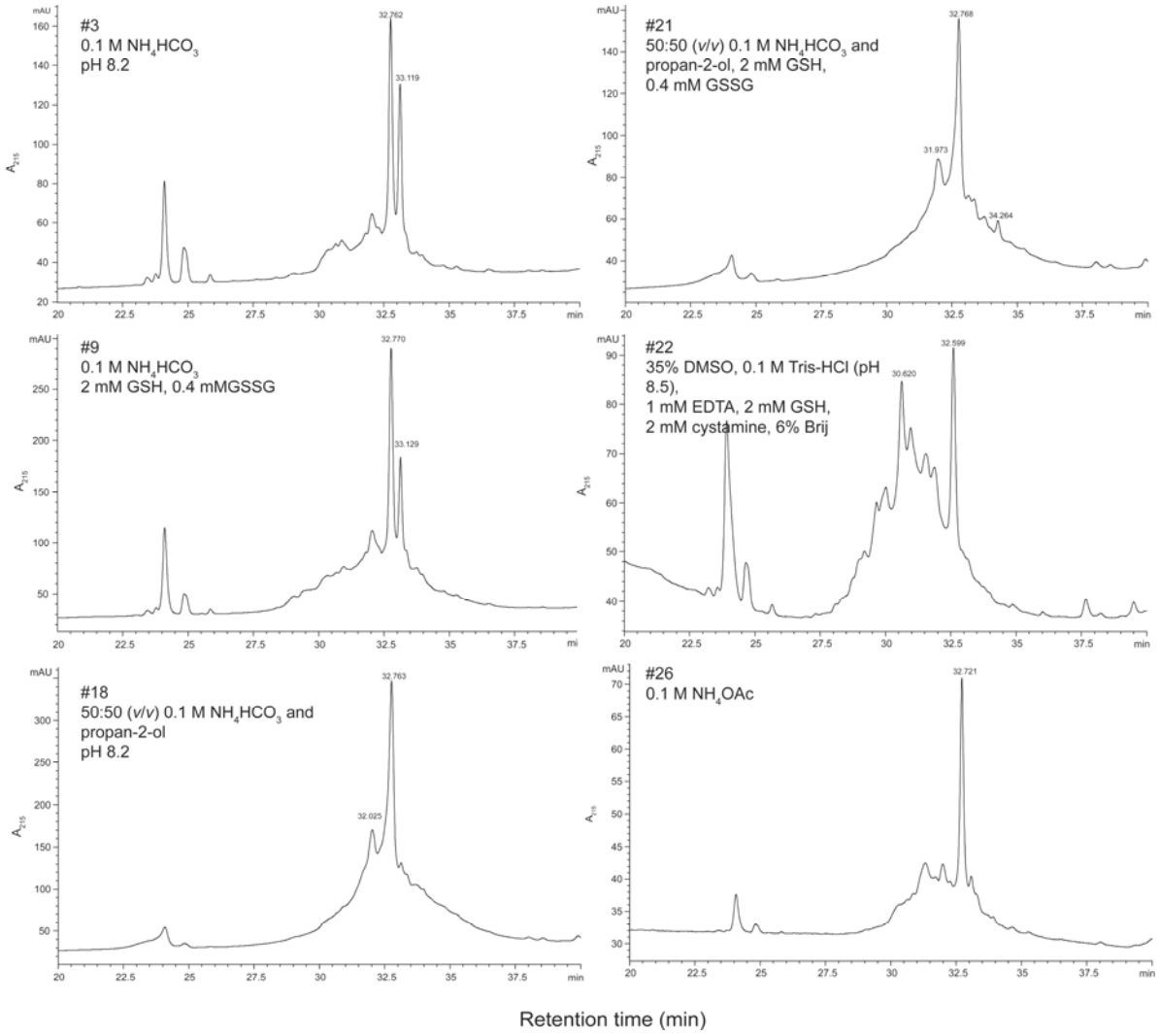

Figure 15: Oxidation trials of kalata B5; condition 3 (top left), condition 9 (middle left), condition 18 (bottom left), condition 21 (top right), condition 22 (middle right), and condition 26 (bottom right). Condition #18 was used for up-scaled oxidation of the peptide.

All the conditions resulted in one major product and several byproducts. Condition 18 gave the highest yield of the major product, and was therefore used for an up-scaled oxidation of the peptide which gave 3.1 mg of pure oxidized peptide.

2.1.2 ^{1}H NMR of the Synthesized Peptide Kalata B5

To check the folding of the major isomer the peptide was analyzed by ^{1}H NMR (Bruker 500 MHz). Comparison of the spectra of this isomer and the natural kalata B5 (extracted from *O.*

affinis) showed different pattern, indicating that the synthetic peptide does not have the native fold and is rather a non-native form of kalata B5 (Figure 16, referred as KB5nn).

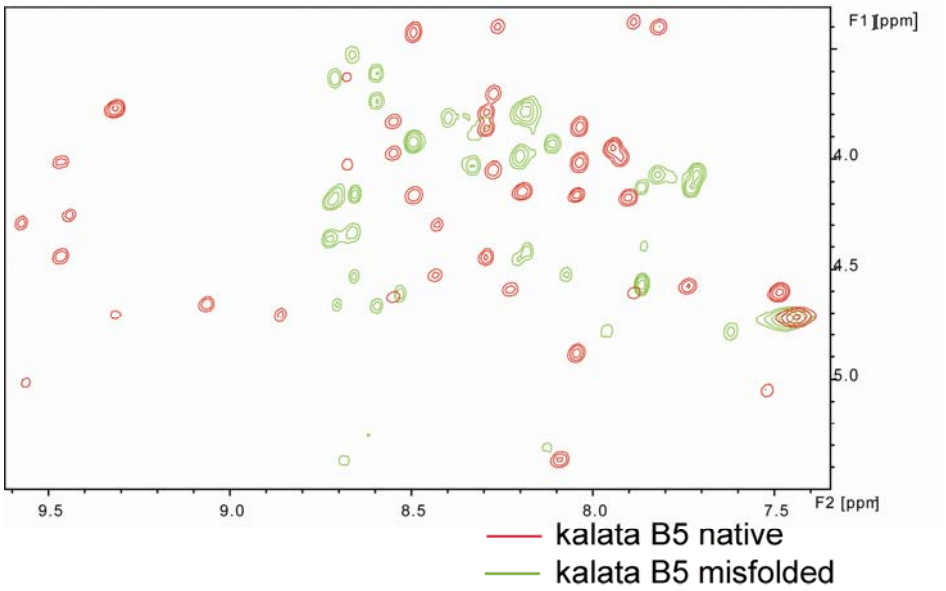

Figure 16: Comparison of the 2D NMR spectra of kalata B5 isolated from O. affinis *aligned with the isomer synthesized in this project. The alignment shows that the two structures have different chemical shifts and is not the same.*

This is the first time a misfolded cyclotide gives a well dispersed spectrum on the NMR. Therefore this represents an excellent opportunity to examine the structure of a misfolded product with the intention to obtain an insight into the factors that may cause misfolding of this peptide with the view to optimize the synthesis. The difference between kalata B5 and kB5nn was confirmed by RP-HPLC which showed that the two peptides had different retention times (Figure 17).

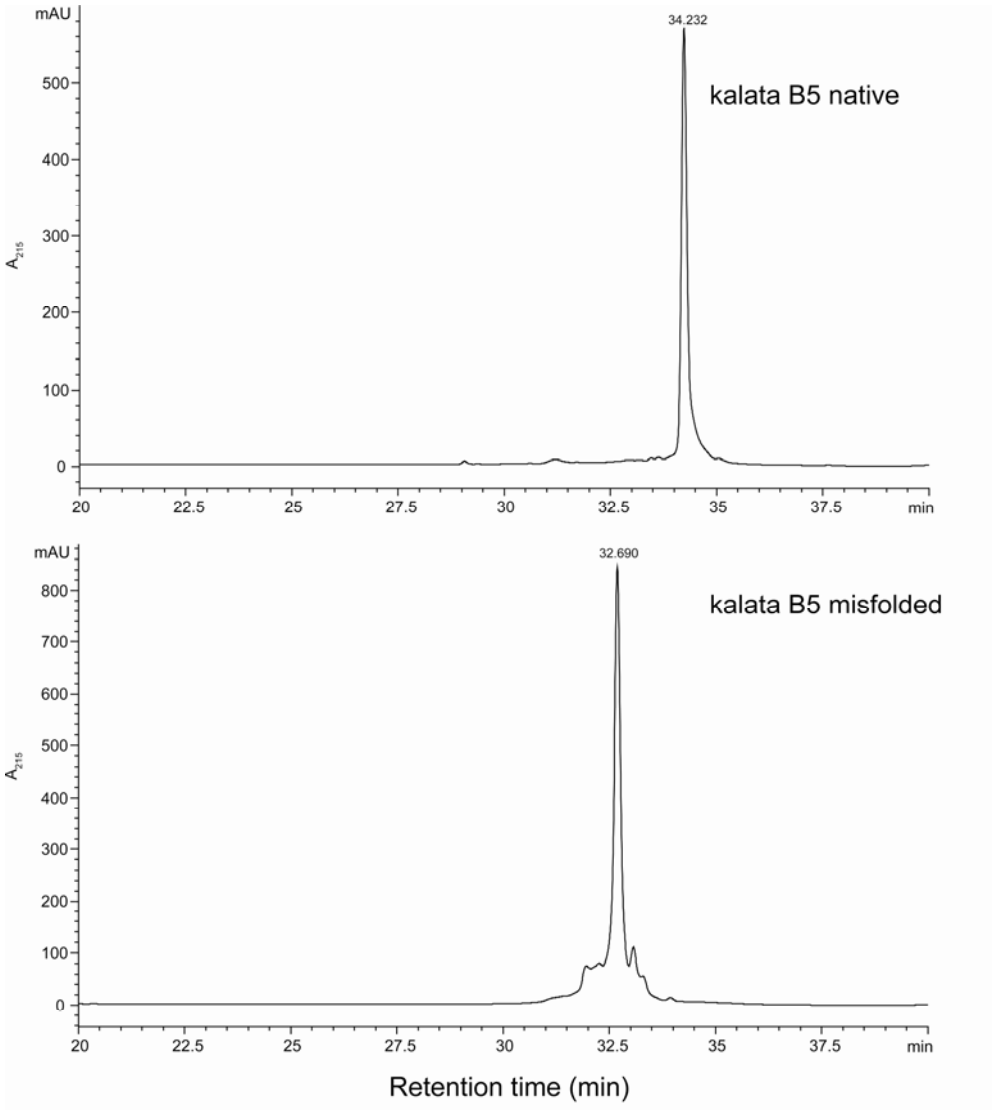

Figure 17: Comparison of the retention times of the naturally occurring kalata B5 and misfolded kB5 (kB5nn) on RP-HPLC.

In a recent paper Aboye et al. also synthesized a bracelet cyclotide, cycloviolacin O2, which resulted in a predominant misfolded peptide, but they managed to rearrange the misfolded form to the native form by using a complex buffer containing a nonionic detergent, 5% Brij 35 (condition 22, Appendix 1). This buffer did not work for our synthetic linear kalata B5. The different chromatograms from RP-HPLC in Figure 15 show a mixture of isomers from the oxidation, but there is no significant peak for the native kalata B5, which has retention time approximately 34.2 min (shown in Figure 17). Condition 21 gave a minor isomer eluting at 34.26 min, which might be the native kalata B5.

In contrast to the cycloviolacin O2 intermediate (CVO2nn) the non-native form of kalata B5 gave well dispersed spectra indicating a rigid well and defined three dimensional structure.

We were not able to solve the disulfide connectivity by reduction alkylation as the partially reduced peptide was impossible to alkylate, but Aboye et al. solved the disulfide connectivity of the misfolded CVO2nn by this method.

The difference between the αH chemical shift observed for kB5nn and that for the same residue in a random coil peptide are the secondary αH chemical shifts. When peptides possess similar secondary shifts it provides a strong indication that the molecular structures of the peptides are much alike. Figure 18 shows a comparison between the secondary αH chemical shifts of kB5nn and CVO2nn and highlights the structural similarity between these peptides. This indicates that the three dimensional structures are much alike and there is a great possibility that the two structures have the same disulfide connectivity. Both CVO2 and kalata B5 consist of 30 amino acid residues and have an extended loop 3 and lysine residues in loop 5 (Figure 3), which are characteristic features of the bracelet cyclotides. Due to lack of NOES in the spectra Aboye et al. were unable to solve the structure of the O2 intermediate. In contrast, our kB5nn gave good quality spectra suitable for structure determination.

2.1.3 Assignment of Spectra

The structure of the kB5nn was determined by recording and assigning 2D NMR spectra. By using the sequential assignment procedure (45) the assignment was straightforward. The individual amino acid spin systems were determined from the TOCSY spectrum by using the NH-NH_{i+1}, Hα-NH_{i+1} and Hβ-NH_{i+1} connectivities acquired from the NOESY spectrum.

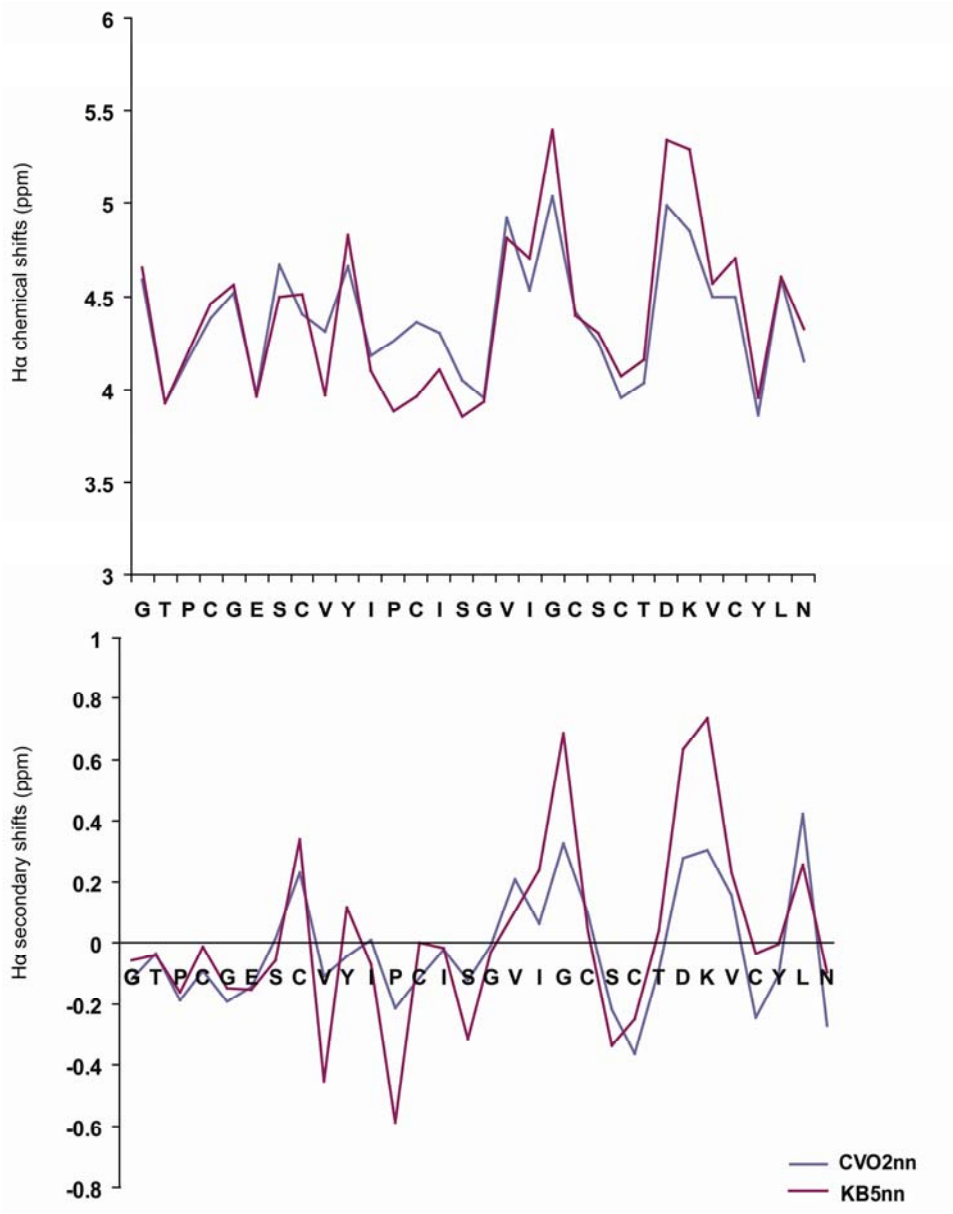

Figure 18: Comparison of the chemical shifts from the NMR data of synthesized kB5nn and cycloviolacin O2 intermediate (CVO2nn). A: The Hα chemical shift values for kB5nn (red) and CVO2nn (blue). B: Secondary shift values for CVO2nn (blue) and kB5nn (red).

2.1.4 Structure Determination of kB5nn

The structure of kB5nn was calculated using 31 dihedral angles. The φ and χ^1 angle restraints were based on coupling constants and NOE patterns, and the calculated restraints are shown in Table 2. $^3J_{H\alpha,\ HN}$ (Hz) was measured from the 1D NMR spectra.

Table 2

Dihedral angle restraints used in structure calculation of kalata B5 non-native

	Dihedral angle restraints	Coupling constants $^3J_{H\alpha,\ HN}$ (Hz)	Amino acid residues
Φ	-120±30	8.0-9.5	Thr2, Cys4, Ser7, Cys8, Ile11, Cys22, Thr23, Val26, Cys27, Tyr28
	105±95		Glu6, Val9, Tyr10, Cys13, Val17, Ile18, Cys20, Ser21, Asp24, Lys25, Leu29, Asn30
	-100±80		Ile14, Ser15
χ^1	-60±30		Glu6, Lys25, Tyr28
	180±30		Tyr10, Cys20, Cys22, Cys 27

The final CYANA run calculated 50 structures, and used the 20 lowest energy structures to produce the structural ensemble shown in Figure 19 a. The structure has a mean RMSD (root mean square deviation) from the average structure of 0.79±0.53Å for the backbone atoms and 1.21±0.47Å for all heavy atoms.

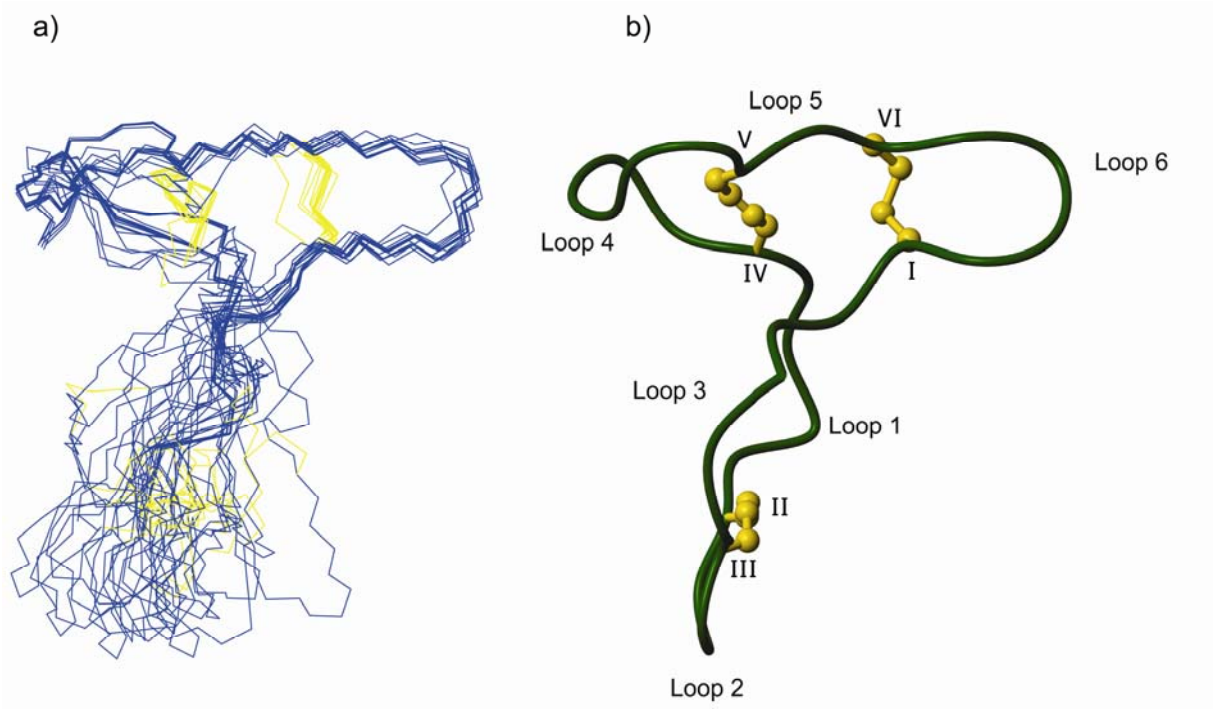

Figure 19: a) The twenty lowest energy structures. The structures are overlaid from residues 12-28. b) Mean structure shown as ribbon representation with the disulfides in ball and stick format. The disulfide connectivity is I-II, III-IV, and V-VI.

The peptide has a region of about ten residues that is quite flexible and hence the RMSD value is quite high for this part of the peptide (Figure 19 a). From residues 12-28 we get more similar alignment for the ensemble of structures Table 3 summarizes the geometric statistics of the 20 lowest energy structures for this well-structured region of the peptide. The region of the structure which is more well-defined shows an extended structure that suggests the presence of two anti parallel β-strands in this part of the molecule. The Hα signals are also shifted downfield in the spectra, which support an extended secondary structure consistent with a β-strand, but due to no hydrogen bonds there is not enough evidence to confirm the β-strands. The disulfide connectivity was adapted from the misfolded CVO2nn, but the three dimensional structure of kB5nn without the disulfides suggested the same connectivity.

Table 3

Structural characteristics of the 20 lowest energy structures of kB5nn

Parameter	
Experimental restraints	
Sequental NOEs	75
Medium range NOEs	15
Long range NOEs	17
Hydrogen bonds	0
Dihedral angles	9
Atomic RMSDs (Å)*	
Backbone atoms	0.79±0.53Å
Heavy atoms	1.21±0.47Å
Ramachandran statistics	
Residues in most allowed regions	53.6%
Residues in additional allowed regions	46.4%

*Atomic RMSDs are the pairwise RMS difference for the family of structures

The peptide is synthesized as linear, but forms the cyclic backbone during oxidation. This reaction (NCL) between Gly19 and Cys20 is described earlier. In Figure 20 the binding of these two amino acids is confirmed by the sequential HN-Hα NOEs between Cys20 and Gly19, indicated on the figure by the black line.

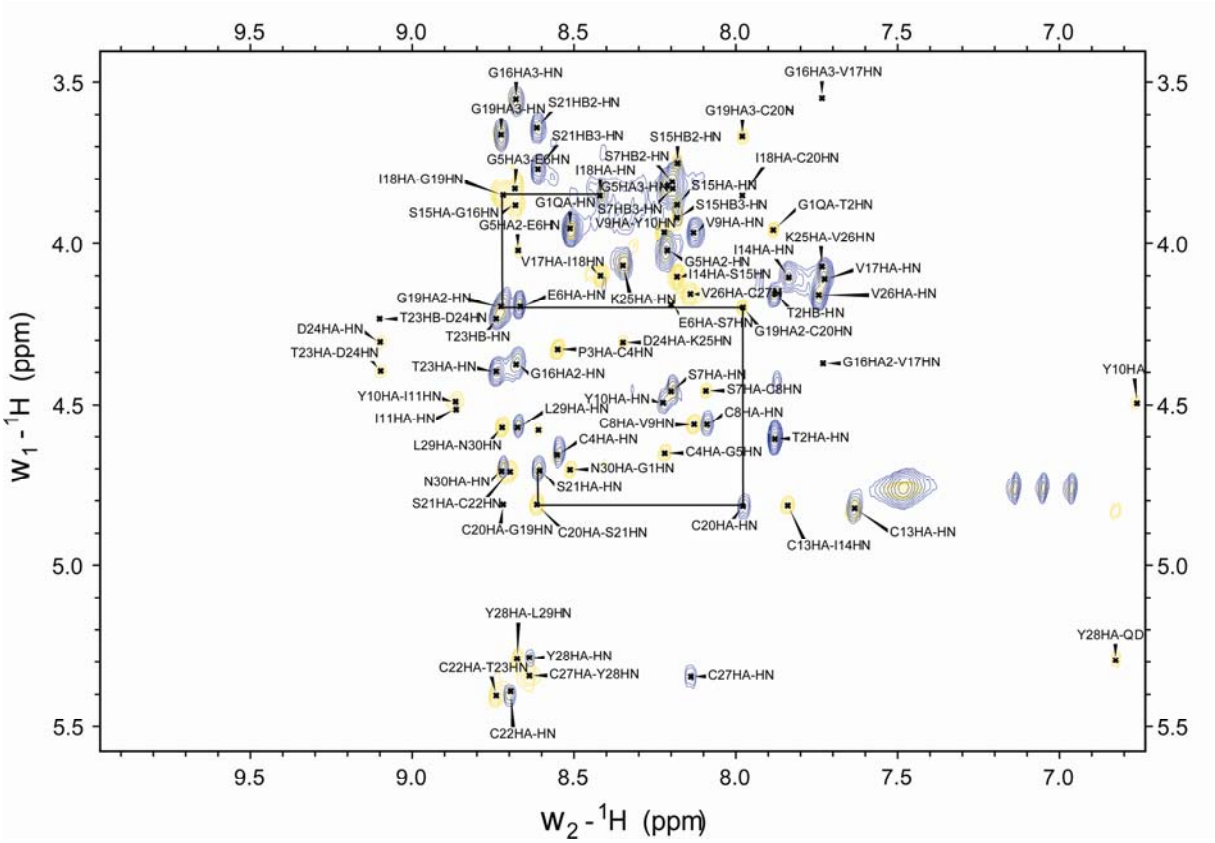

Figure 20: The NOESY and TOCSY spectra showing the assignment of NH-Hα of all the residues in kB5nn. The line is showing the continuous assignments through the region where the cyclization has happened; from residue G19-C20.

The surface structure of kB5nn (Figure 21) show hydrophobic residues in green close together and charged residues in red and blue gathered on the surface pointed out in the solvent. The way these residues have clumped together, due to their properties, is probably the reason why the molecule has stabilized in this conformation. This kind of positioning seems to happen with other misfolded bracelets as well. The glutamic acid (Glu6) is important for the stabilized cyclotide fold as the amino acid is situated in the core of the molecule and forms hydrogen bonds with the surrounding amino acids (46). Figure 21 illustrates that the misfolded form of kalata B5 has this glutamic acid pointing out in the solvent.

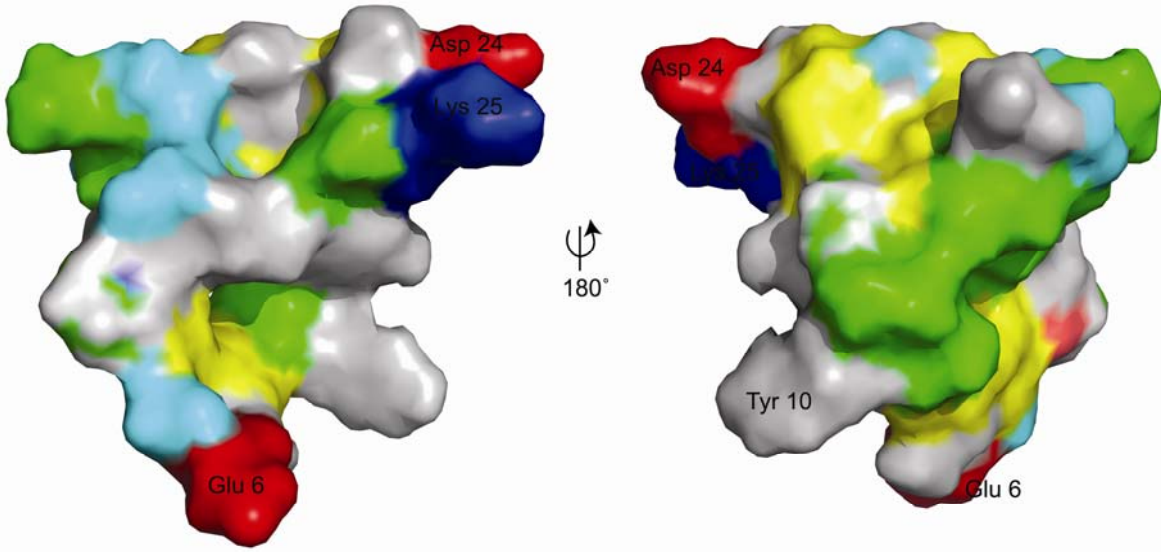

Figure 21: The surface structure of kalata B5 non-native; the green parts showing hydrophobic regions, the yellow showing the cysteines, the light blue showing glycines, the red showing negatively charged residues, and the blue showing positively charged residues.

2.1.5 Insecticidal Activity of Kalata B5

Kalata B5 was tested for insecticidal activity because previous reports suggested that this bracelet cyclotide would be 10-fold more potent than kalata B1 (unpublished data). *H. armigera* were divided up in three groups of four larvae each and fed an artificial diet where one group had a diet supplemented with kalata B5. For comparison another group was fed a diet supplemented with kalata B1 and the last group was a control group with no supplements. The mortality rate and growth were measured over 90 hours. In the last day the remaining diet and the frass produced by the larvae were also measured.

As it was not possible to produce kalata B5 synthetically due to the accumulation of the non native misfolded product, kalata B5 and B1 used in these trials have been extracted from aerial parts of *O. affinis* using efficient strategies for extraction (12) (provided by Dr Josh Mylne, Crystal Huang and Dr Manuel R. Plan).

Our data show that kalata B1 is more potent as an insecticidal than kalata B5. The larvae in the group of controls grew to a final weight of 17.4 mg whereas the treated populations grew

to 15.2 mg and 22.4 mg for kalata B1 and kalata B5, respectively. Mean weight difference after 90 hours of feeding was 16.0 mg, 12.3 mg and 18.7 mg for the control group, kalata B1 group and kalata B5 group, respectively. Figure 22 shows the mean percentage weight difference over time for the different groups in the trial. One larva in the group feeding on the kalata B5 diet was large and grew significantly more than the other larvae in the treatment. By removing the numbers for this particular larva the mean numbers for the two groups of kalata B1 and kalata B5 were quite similar. Final weight is then 15.6 mg for the kalata B5 group and mean weight difference 12.9 mg. 250 mg of diet was prepared, and they ate in average 77% of their diet. A t-test gave p-values >0.5 for the comparison between all the groups and shows that there was no significant difference between the groups as the number of replicates was too low.

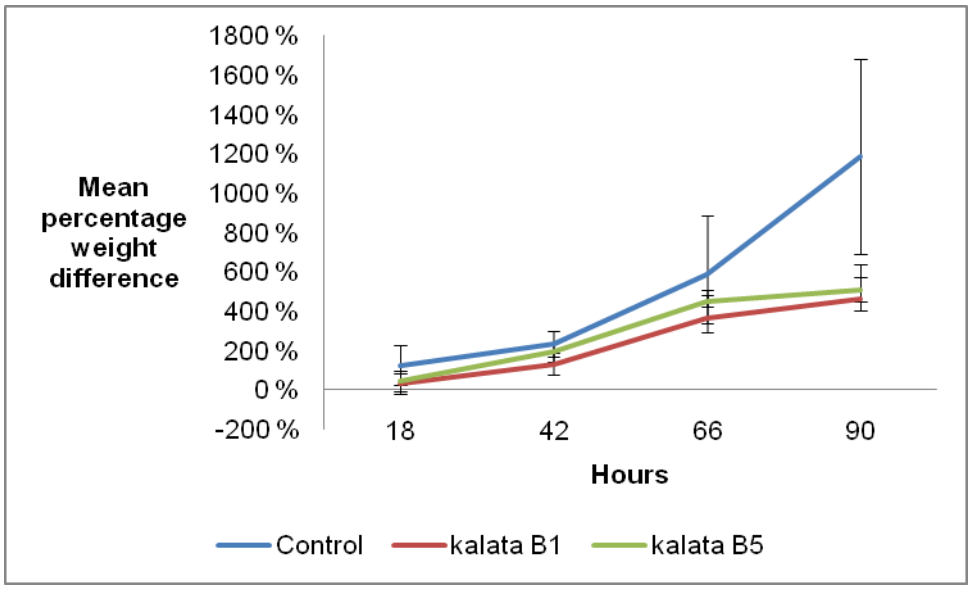

Figure 22: The percentage weight difference of the larvae during 90 hours of feeding trials. The control group (blue), kalata B1 group (red) and kalata B5 group (green).

In contrast to what has been reported earlier the larvae which were fed kalata B5 had the highest number in mean weight gain (Table 4).

Table 4

Mean weight difference, mean diet consumed, and mean amount of frass produced after 90 hours of feeding trials with *H. armigera* (mg)

	Mean weight difference after 90 hours	Mean diet consumed	Mean amount of frass produced
Control	16.0±1.3	195.3±1.8	7±1
Kalata B1	12.3±2.8	182.9±5.3	7.7±2.4
Kalata B5	18.7±10.3	202.7±13.6	14±3.6

2.2 Conotoxins

2.2.1 Design and Synthesis of Three Analogues of cPVIIA

PVIIA is a potent potassium channel blocker which suffers from *in vivo* degradation. In this study I have attempted to synthesize a cyclic version of PVIIA by adding a linker between the N and C terminal of the peptide chain. With a distance between the N and C termini of PVIIA of 12.6 ± 0.29 Å (estimated from the three dimensional structure of PVIIA), molecular modeling techniques calculated the number of residues in the linker to be four or more. Fewer than four residues in the linker will cause restraints in the molecule. Based on the calculated data three cyclic analogues of PVIIA were designed, with the following linker sequences: TRNG (PVIIA4), GGAAGG (PVIIA6) and GGAAGAG (PVIIA7) (Figure 10). All linker calculations were done by Dr Richard Clark. Three analogues of PVIIA were synthesized manually using Boc-chemistry SPPS. The average yields of the coupling reactions were 99.6%, 99.3% and 99.8% for PVIIA4, PVIIA6 and PVIIA7, respectively. After the chain assembly was completed, the N-terminal Boc group was removed with TFA, and the resin washed with DMF and DCM and dried under a nitrogen atmosphere. About 500 mg of the resin was cleaved using HF/*p*-cresol/*p*-thiocresol (18:1:1 *v*/*v*/*v*) at -5-0˚C for 1.5 hour. The residual HF was evaporated, and the crude peptide was washed with cold diethyl ether, dissolved in 50% acetonitrile containing 0.1% TFA and lyophilized. The crude peptide was redissolved in 0.05% TFA (buffer A), and analyzed by RP-HPLC and ES-MS.

Several oxidation conditions were examined for the linear fully reduced peptide (Appendix 1, conditions 1-6 and 8) and they all yielded a mixture of isomers. Figure 24 shows that condition 3 produced the highest yield of the major isomer, which was believed to be in the native form.

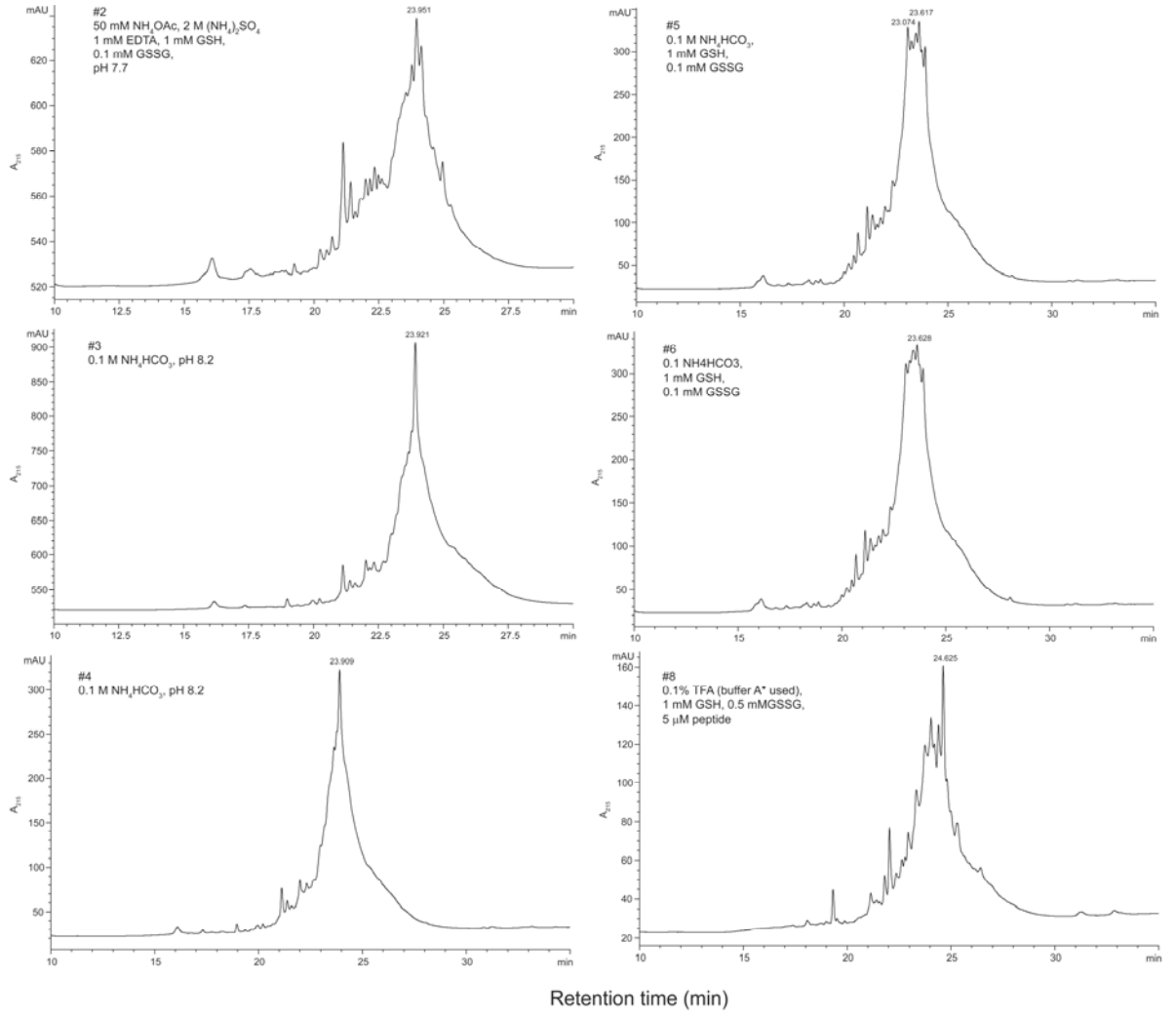

Figure 23: Oxidation trials of PVIIA7. Condition 2 (top left), condition 3 (middle left), condition 4 (bottom left), condition 5 (top right), condition 6 (middle right), and condition 8 (bottom right)

To limit the number of possible isomers to three, the peptides were synthesized with Acm protecting groups for Cys III and Cys VI. The Acm protecting groups will still be attached to the cysteines after the HF cleavage whereas the other cysteines which are synthesized with MeBzl protecting groups will have their MeBzl groups released during HF cleaving. Therefore will only Cys I, Cys II, Cys IV and Cys V form disulfides during the oxidation, and possible disulfide connectivities are shown in Figure 25.

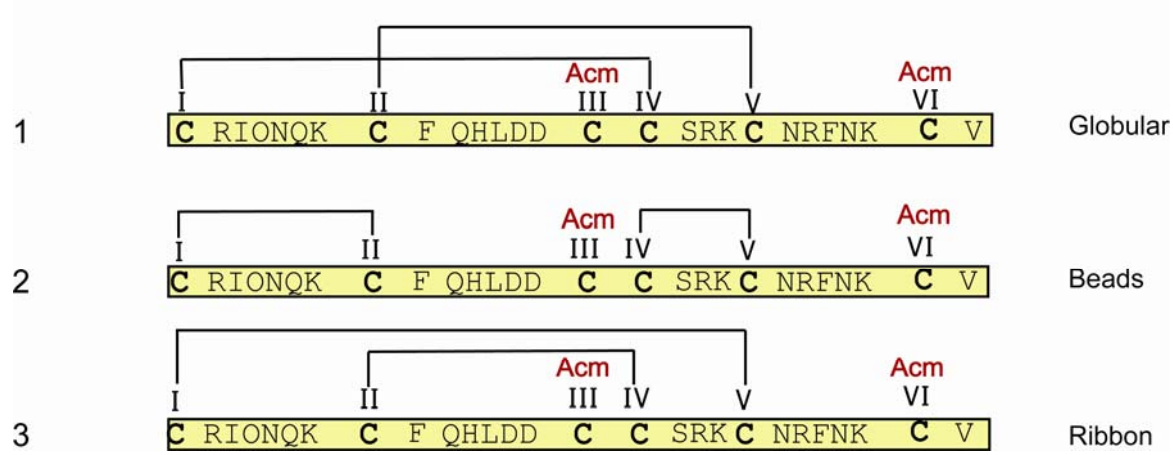

Figure 24: The different isomers of disulfide connectivities that can be obtained after the first step oxidation. The globular form of the disulfide connectivity is the native form.

Another oxidation step is necessary to oxidize the Acm protecting cysteines, Cys III and Cys VI; the iodine oxidation. This method will simplify the purification and identification, but the disadvantage of this method is that the Acm protecting groups may limit the native folding of the peptide since one of the disulfides are predetermined. If all the cysteines are protected by MeBzl as many as 15 isomers may form during the oxidation, which will make it more difficult to isolate the native one.

The partially oxidized peptide was fully oxidized with iodine and the Acm protecting cysteines would form the last disulfide. RP-HPLC and ES-MS analyses confirmed the major product to be fully oxidized. Purified cPVIIA4, cPVIIA6 and cPVIIA7 were analyzed by ^{1}H NMR to check the folding. All three analogues gave poorly dispersed ^{1}H NMR spectra (Figure 26), indicating a lack of a well ordered three dimensional structure.

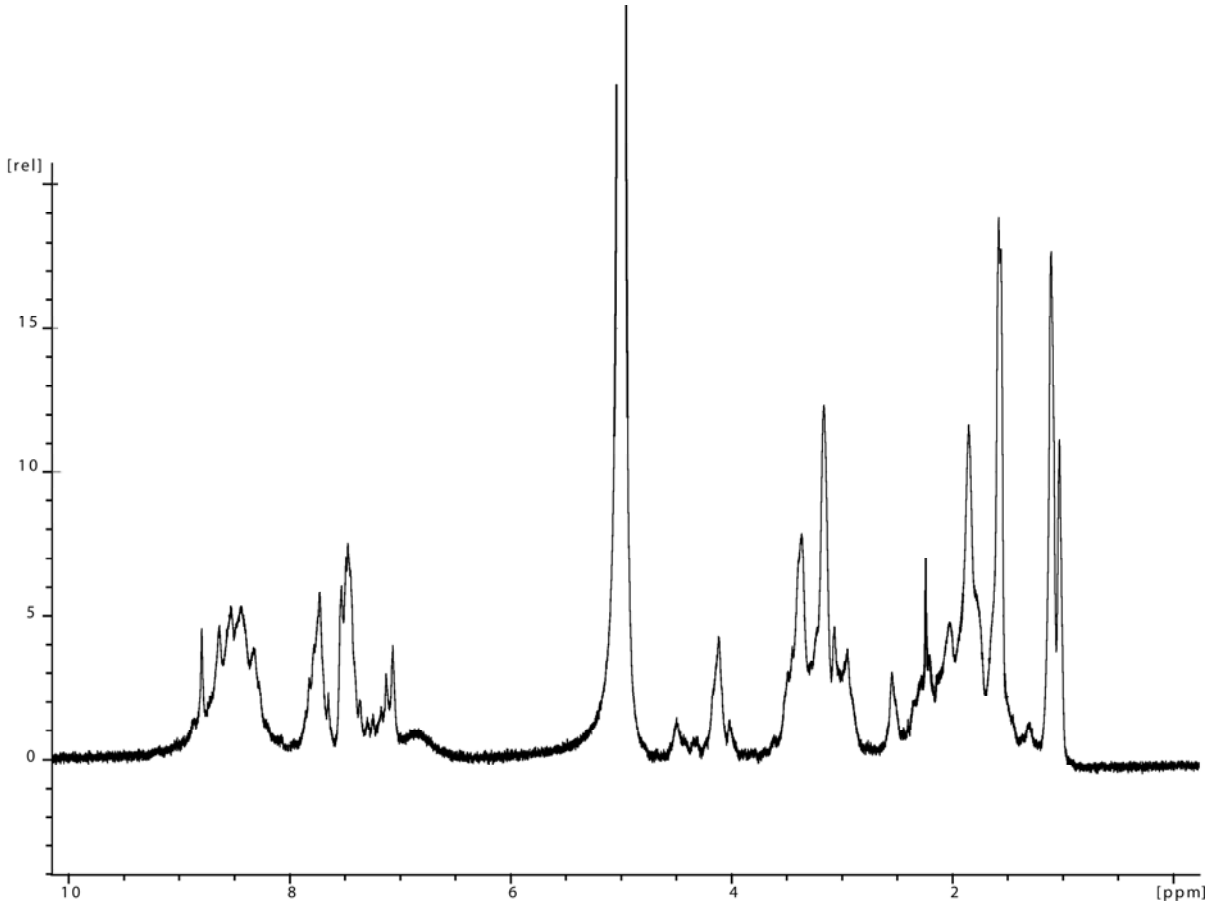

Figure 25: ^{1}H NMR spectra of the one of the cPVIIA7 analogue showing a poorly dispersed spectra, indicating a product which is not folded. The lack of peaks in the region of 9-11 ppm indicates a not folded product.

2.2.2 Synthesis of cPVIIA (without Acm Protecting Groups)

The Acm protected Cys residues could have limited the native folding of the peptides. PVIIA7 was therefore synthesized again, but with no Acm protected Cys residues this time. The possible isomers after the oxidation will then be 15. Average coupling yield was 99.8%. After purification and oxidation with condition 3 (Appendix 1.), the folding was analyzed by ^{1}H NMR, but the spectra showed poor dispersion of NMR signals which is indicative of a misfolded peptide.

Comparison of the retention times of the newly synthesized PVIIA7 with only MeBzl protecting cysteines and the PVIIA7 with two Acm protected cysteines show that the peptides have approximately the same retention times, indicating similar misfolded peptides.

When NCL is used the cyclization is the fast step in the reaction and the formation of disulfides is the rate limiting step. When the cyclic backbone of the peptide is made first it may limit the native folding since the cyclic peptide will not be as flexible as the linear one and the positions where the disulfides form is probably harder to make because of restraints.

2.2.3 Synthesis of PVIIAs7 without the Thioester Linker

The last attempt to make PVIIA fold properly into to the native form was to synthesize the peptide without the thioester linker. Now the linker of Gly and Ala residues were split and attached to both termini; GAGG was added on the N terminus and GAG on the C terminus. Since we had not been able to form the native folding of PVIIA so far it was decided to attempt a strategy where the disulfides were formed first and then the cyclization reaction would be performed. The difficulty in this approach is that as the cyclization is a simple amide bond formation other unwanted side reactions may occur e.g. reactions between the side chains to the termini or intermolecular reactions which form dimers. PVIIA has three lysines and two aspartic acids whose side chains can also form amide bonds.

The synthesis was conducted with Microwave-assisted (CEM Microwave Peptide Synthesizer with PepDriver software) Fmoc SPPS. After cleavage with TFA, the crude peptide was purified by RP-HPLC with a 1% linear gradient of buffer B in buffer A (Figure 27).

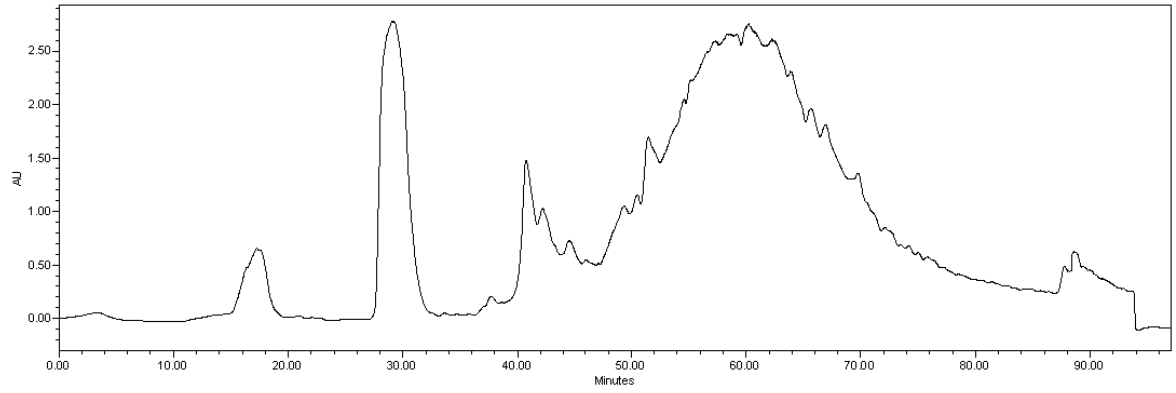

Figure 26: RP-HPLC of crude PVIIAs7 (-thioester linker).

Several oxidation trials of PVIIAs7 were conducted (Appendix 1, condition: 1-4, 7-8, 11-17, 19-20, 22-23, 26-27, 29-30, 35-44) and analyzed on the analytical HPLC. Condition 29 (0.1 M NH4OAc, 1mM GSH, 0.1mM GSSG, pH 7.9 at 4˚C for 24 hours) seemed to be the one with the best yield from the intensities of the peaks (Figure 28), and was used in up-scaled oxidation of the peptide. Approximately 1mg of the pure folded linear PVIIAs7 was prepared for NMR data analysis by dissolving it in 500µL H_2O and 50 µL D_2O. The spectra from ^1H NMR shows well dispersed peaks in the area of 9-11 ppm which confirms the folding of peptide (Figure 29).

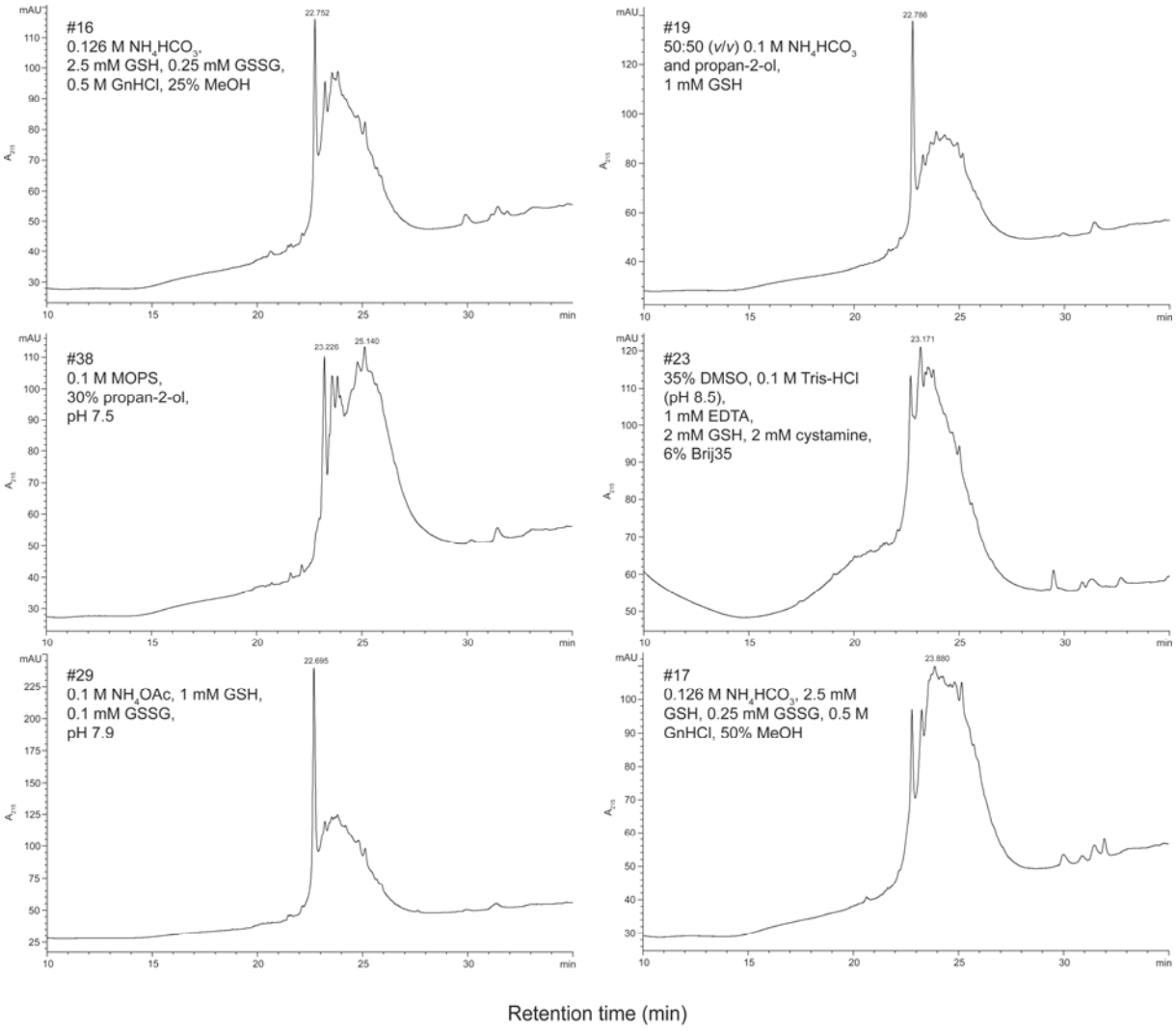

Figure 27: Some examples of the oxidation conditions examined for PVIIAs7; condition 16 (top left), condition 38 (middle left), condition 29 (bottom left), condition 19 (top right), condition 23 (middle right), and condition 17 (bottom right).

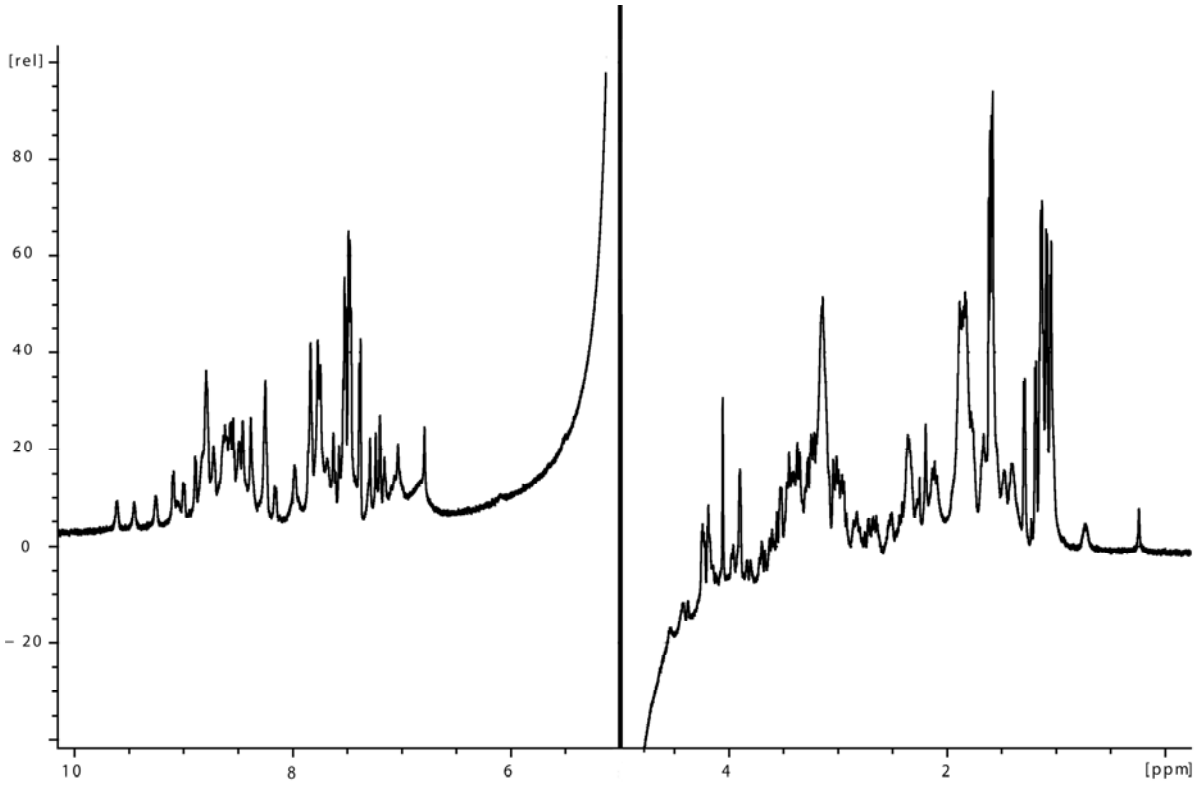

Figure 28: [1]H NMR spectra of linear PVIIAs7. A well dispersed spectra showing that the peptide has folded. The dispersed peaks in the region of 9-11 ppm confirm the folding.

2.2.4 [1]H NMR Resonance Assignments of Linear PVIIAs7

The spin systems for the individual amino acids from the TOCSY spectrum were identified and assigned to specific residues in the sequence using the NH-NH_{i+1}, Hα-NH_{i+1} and Hβ-NH_{i+1} connectivities from the NOESY experiments. Secondary chemical shifts (Figure 30) for the backbone Hα protons were calculated using the measured chemical shifts and the random coil values. Comparison of the Hα chemical shifts and the Hα secondary chemical shifts between the synthetic linear PVIIAs7 and the isolated linear PVIIA from *C. purpurascens* (33) show that the structures are quite similar and thus possess similar three dimensional structures.

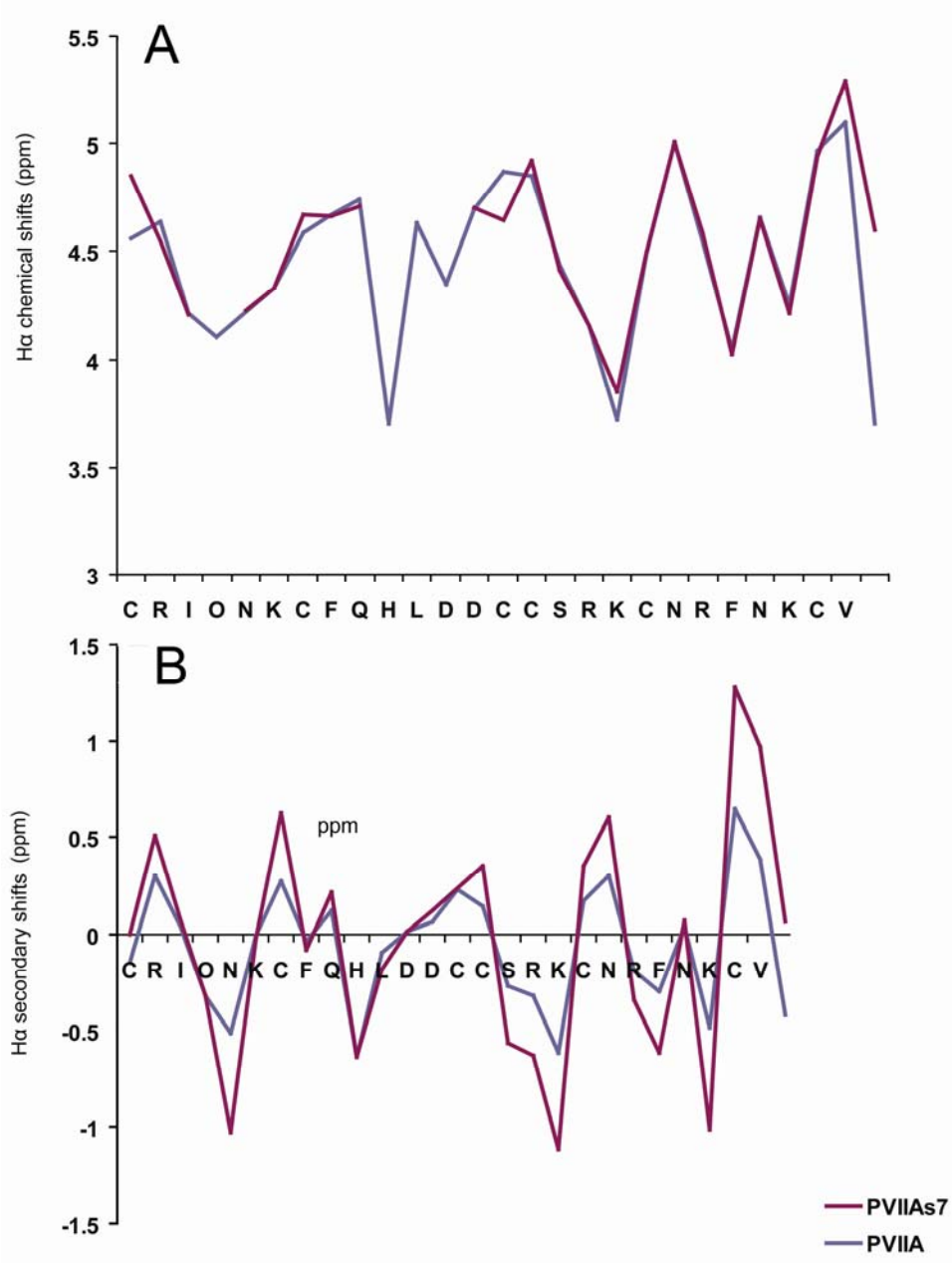

Figure 29: A: Hα chemical shifts for isolated PVIIA from C. purpurascens *(blue) and synthesized linear PVIIAs7 (red). B: Values of secondary shifts for isolated PVIIA from* C. purpurascens *(blue) and synthesized linear PVIIAs7 (red). The values for each peptide are almost identical indicating that the three dimensional structures are very similar, which they are supposed to be.*

2.2.5 Cyclization of the Linear PVIIAs7

Three different methods were tested to find the optimum conditions to cyclize the linear folded PVIIAs7. Because the glycines on each terminus of the linear peptide are achiral they will form only one isomer no matter how they are approaching each other in the reaction. These coupling agents were attempted in the following concentrations:

i) HBTU and DIPEA in DMF

   a. 739 and 2264 molar peptide equivalents, respectively, in 150µL DMF (peptide concentration of ~0.7 mg/ml)

   b. 18.5 and 3629 molar peptide equivalents, respectively, in 183 µL DMF (peptide concentration of ~0.6 mg/ml)

ii) PyBOP and DIPEA in DCM

   a. 2 and 10 molar peptide equivalents, respectively, in 3 ml DCM (peptide concentration of ~0.03 mg/ml)

   b. 7 and 227 molar peptide equivalents, respectively, in 0.5 ml DCM (peptide concentration of ~0.2 mg/ml)

   c. 21 and 680 molar peptide equivalents, respectively, in 1.5 ml DCM (peptide concentration of ~0.07 mg/ml)

   d. 142 and 4536 molar peptide equivalents, respectively, in 100 ml DCM (peptide concentration of ~0.01 mg/ml)

iii) HOBt and EDC in DMSO

   a. 20 and 60 molar peptide equivalents, respectively, in 3 ml DMSO (peptide concentration of ~0.03 mg/ml)

   b. 27 and 209 molar peptide equivalents, respectively, in 0.5 ml DMSO (peptide concentration of ~0.2 mg/ml)

   c. 82 and 628 molar peptide equivalents, respectively, in 1.5 ml DMSO (peptide concentration of ~0.07 mg/ml)

The reaction with HBTU and DIPEA in DMF was quenched with 10 µL of TFA after approximately 1 min. The reaction mixtures with PyBOP/DIPEA and HOBt/EDC were stirred at room temperature (22˚C) for approximately 12 hours and approximately 18 hours, respectively.

The progress of the cyclization reactions were monitored by ES-MS and analytical RP-HPLC on a C18 column (Phenomenex, 250 x 4.60 mm 5 micron, 300 Å pore size, 5µm particle size) using a 2% linear gradient of buffer B in buffer A at a flow rate of 1 ml/min. The different masses of reduced or oxidized PVIIAs7 are shown in Table 5.

Table 5

The different masses of PVIIAs7 during oxidation

	Mass (g/mol)	M+2 (m/z)	M+3 (m/z)	M+4 (m/z)	M+5 (m/z)
Linear reduced PVIIAs7	3703	1852.5	1235.3	927.8	741.6
Linear oxidized PVIIAs7	3697*	1849.5	1233.3	925.3	740.4
Cyclic oxidized PVIIAs7	3679**	1840.5	1227.3	920.8	736.8

*The linear folded peptide will have 6 masses less than the non-folded one, corresponding to the loss of 6 H.
**The cyclic folded peptide will have 18 masses less than the linear folded peptide, corresponding to the loss of H_2O during the amide bond formation.

Method i), which involved the HBTU and DIPEA in DMF, did not appear to be efficient. RP-HPLC analysis of the reaction mixture showed several peaks, but the desired cyclic product was absent. ES-MS analysis of the peaks did not identify the mass of cPVIIA7, but a number of unidentified masses of what must be different side reactions. The concentration of the coupling agents were changed (i b), but there were no sight of a cyclic PVIIAs7. By taking ES-MS analyses between the adding of the different coupling agents we saw that the peptide disappeared.

The peptide did not manage to cyclize with method ii) either. With the lowest concentration of the coupling agents (ii a) there was hardly observed any peaks at all, and the few peaks which were collected were not concentrated enough to show any masses at all on the ES-MS analyses. With higher concentrations of the coupling agents (ii b, c and d) a major peak eluted after approximately 38 min (Figure 31, peak B) and the ES-MS of the peak show masses of what might be a polymeric byproduct of the reaction (Figure 32).

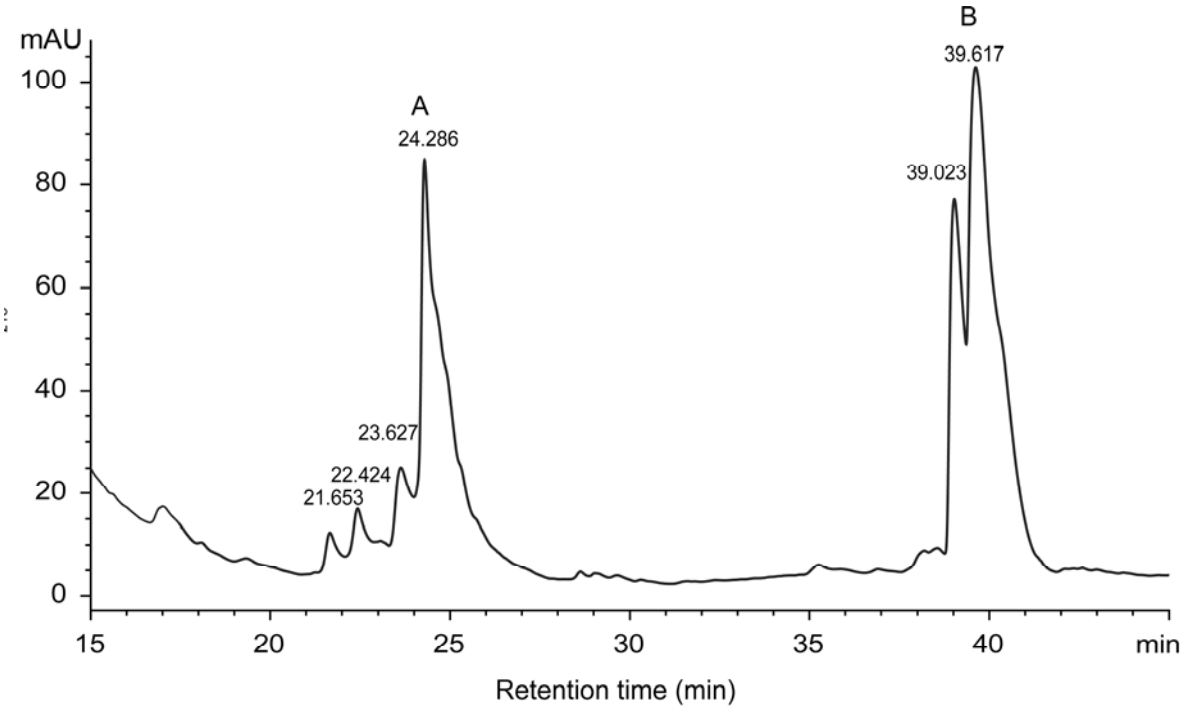

Figure 30: Attempt to cyclize PVIIAs7 with method ii b). Two major peaks are eluted. A: the linear peptide, B: a byproduct of PVIIAs7.

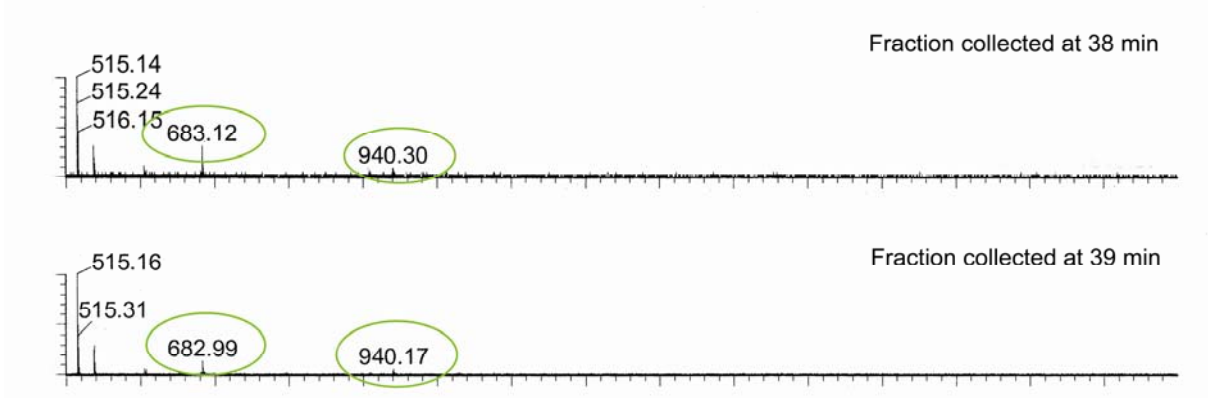

Figure 31: The ES-MS of peak B in Figure 31. The masses have not been identified to a specific product.

The linear PVIIAs7 was also identified on the ES-MS with a retention time of approximately 24 min (peak A), but there were no masses identified of cPVIIA7. Dimerization of the peptide and reactions between the side chains are more likely to happen when the peptide concentration is high. In the very last attempt was the peptide concentration made really low (ii d) to avoid the intermolecular reactions, but still there was several polymeric byproducts produced (data not shown), which have not yet been identified due to time restraints.

With method iii) a major peak eluted approximately 30 min (Figure 33, peak B), but the ES-MS analysis of the peak did not show any mass of interest (Figure 34).

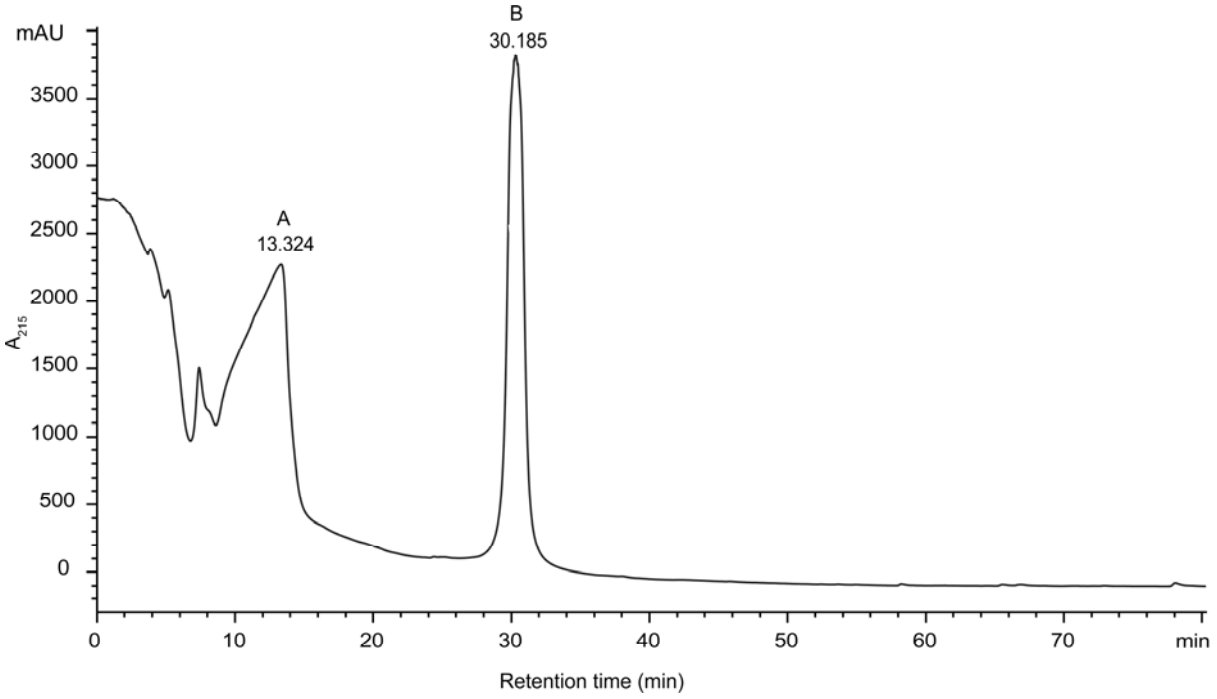

Figure 32: The RP-HPLC trace of the cyclization reaction of PVIIAs7 with method ii). One major peak elutes at 30 min. The peak eluted at 13 min is the reaction agents.

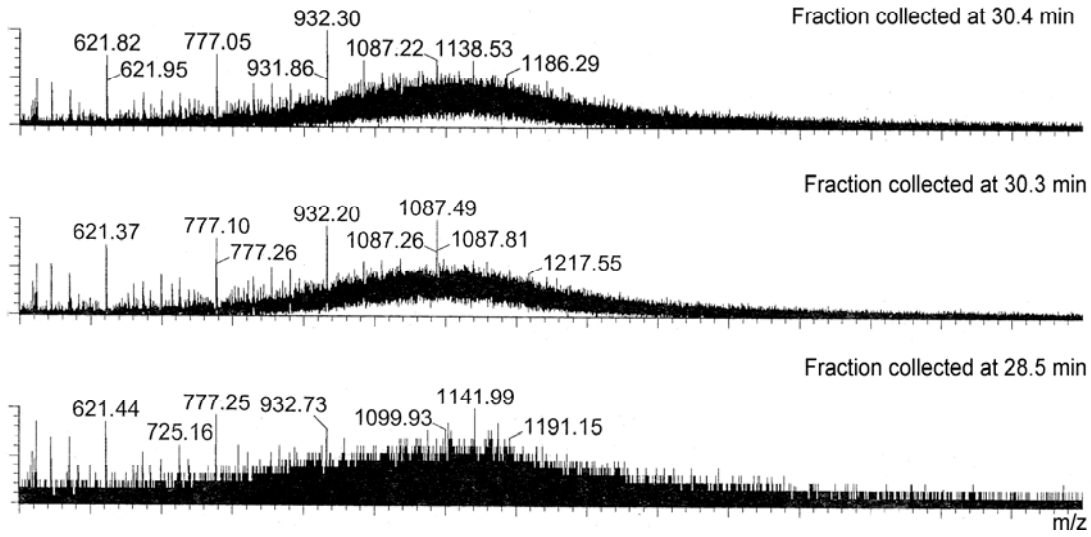

Figure 33: ES-MS of peak B in Figure 33. The spectra show a mixture of several masses that are the masses of different byproducts from the reaction.

The fractions from the time period where the linear PVIIAs7 usually elutes (approximately 24-27 min, Figure 35) showed some very, weak signals on the ES-MS of the correct masses of cPVIIA7 (Figure 36). The intensity was too low to draw any conclusions from the ES-MS analyses and the amounts were too small to isolate anything of the wanted peptide.

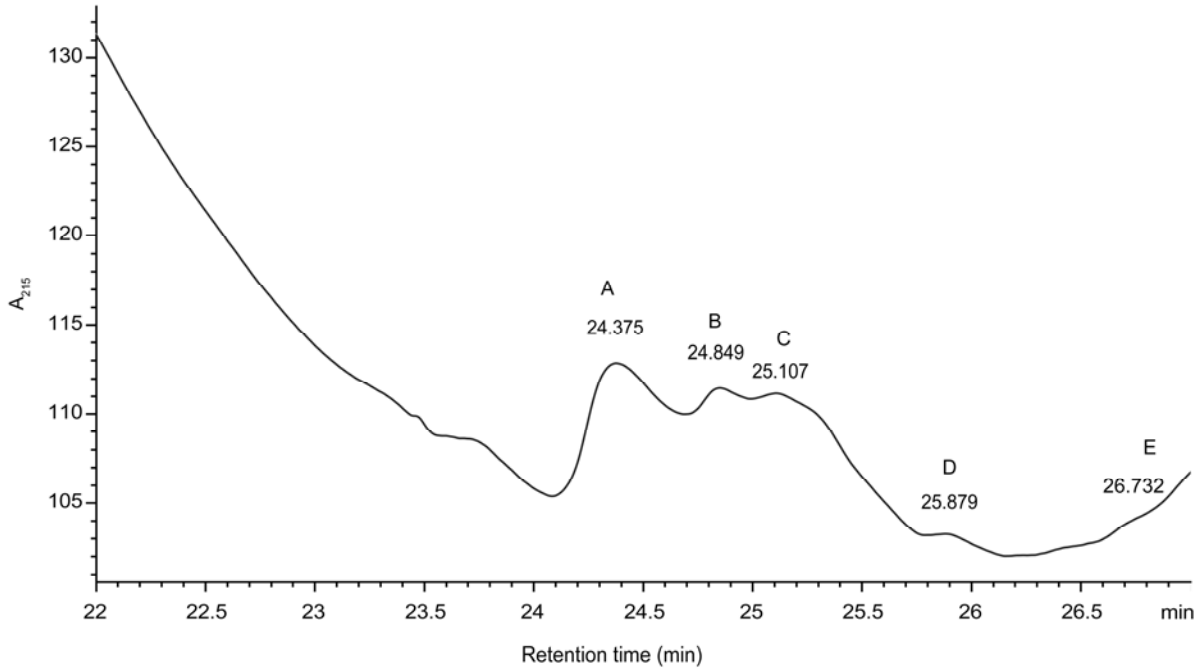

Figure 34: The RP-HPLC trace from Figure 33 with the range 22-27 min. Some minor peaks were identified by ES-MS as shown in Figure 37 and Figure 36.

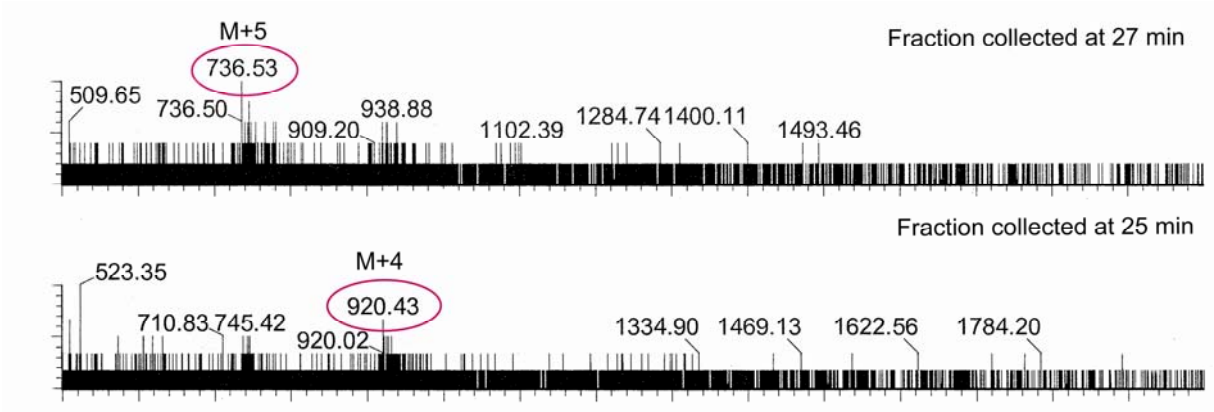

Figure 35: ES-MS of peak D and E in Figure 35. The masses match the mass of a cyclic PVIIAs7.

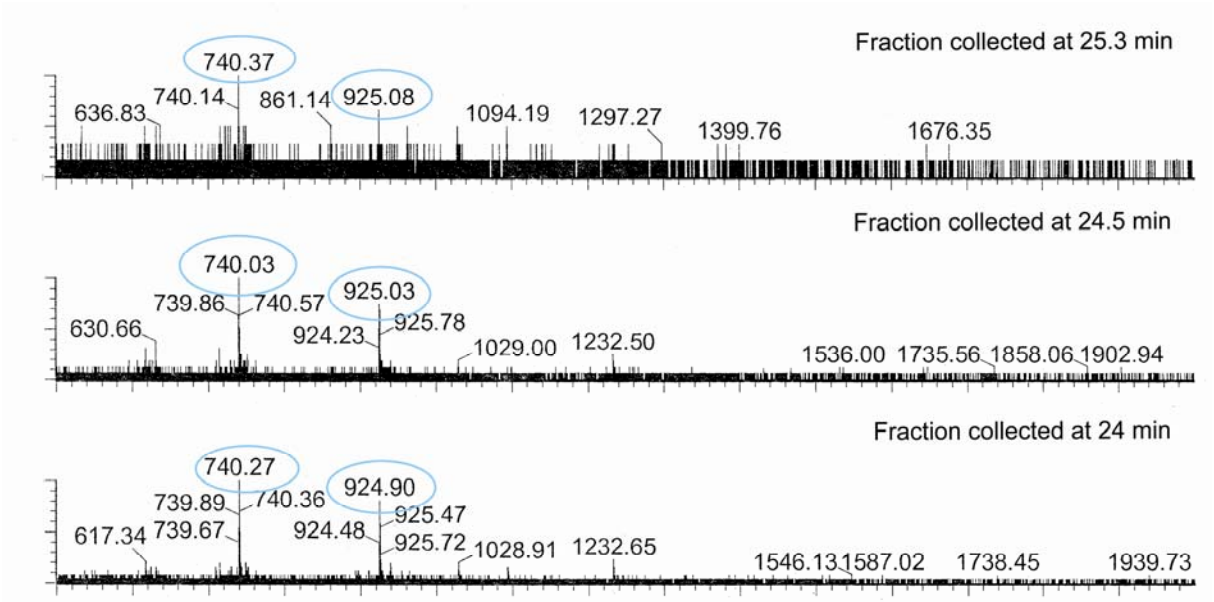

Figure 36: The masses of the linear PVIIAs7 were identified by ES-MS of peaks A, B and C in Figure 35.

3 Discussion

3.1 Cyclotides

3.1.1 Synthesis and Oxidative Folding of the Plant Cyclotide Kalata B5

The extraordinary stability and sequence variability possessed by the cyclotides, together with their potent and diverse bioactivities suggest that these cyclic peptides are ideal scaffolds for the generation of stable protein-based drugs and as potential drug leads in agriculture and biotechnology. The CCK is an attractive scaffold for engineering proteins because it causes the ultrahigh stability of the protein. However, to fully exploit the system of the CCK we need to understand the properties of the scaffold. The bracelet subfamily, which is the major part of the cyclotides, has, due to a lack of a synthetic methodology, been excluded from being used as drug design templates. Before the framework can be fully exploited and the structural diversity can be available by synthesis, it is of great importance that the most efficient folding condition for bracelet cyclotides is found.

Kalata B5 was synthesized and oxidized as described in the previous section, but ^{1}H NMR comparison to the natural isolated kalata B5 showed different spectra. A non-native form of kalata B5 was made and identified as a predominant folding product in the RP-HPLC analyses of the folding mixture. The cyclic backbone, together with the formation of the three disulfide bonds are features that define the topologically complex CCK motif and folding of this has proven to be quite challenging. A number of possible folding conditions from the literature were evaluated, but the misfolded isomer gave the highest yield in most of the different oxidation conditions (Figure 15). Since the cyclotides have 3 disulfides, there are 15 possible isomers produced after an oxidation. As a result, an oxidation often results in a misfolded form. However, since the misfolded peptide had a well dispersed NMR spectrum, the structure was able to be determined. Studying the structure of a misfolded peptide can give vital information about why the misfolding happens and provide useful knowledge for future work with the bracelet cyclotides. Due to their extraordinary stability, the cyclotides have the potential to be used as scaffolds for bioactive sequences that can be grafted into the cyclotide backbone. Of all the cyclotides characterized so far, 70% are from the bracelet subfamily, and until now it has been difficult to make these peptides fold into their native

form. Like the synthesis of kalata B5, the synthesis of CVO2 also ended in a misfolded product. This was solved using a complex buffer system. Unfortunately this same buffer was ineffective in the folding of kalata B5. With retention time of approximately 34 min, a possible native form of kalata B5 was recognized in condition 21 with 50% propan-2-ol (a classical folding mixture for cyclotides). For further work with folding of kalata B5 I would suggest investigating this buffer condition closer and try optimizing it with different concentrations of reduced and oxidized glutations, different incubation times and different temperatures. Other organic solvents, like methanol or DMSO, can also be tested. According to previous reports, nonionic detergents can improve the oxidative folding of disulfide rich hydrophobic peptides (47). Brij 35 was examined in this project, but did not fold our peptide. Tween 40 and Tween 60 are other detergents that can be studied. For an up-scaled synthesis of bracelet cyclotides for commercial use, the folding issues must be solved. It is therefore essential that the structure of kB5nn is examined.

3.1.2 Structure Determination of Non-Native Kalata B5

The structure of the misfolded product of the original synthesis of kalata B5 was determined. A comparison of the Hα chemical shifts and the Hα secondary shifts of kB5nn and another misfolded bracelet cyclotide, CVO2nn, showed quite similar values. This indicates similar three dimensional structures. Structural determination of kB5nn showed that it had a flexible region in the molecule. Distance restraints suggested the existence of two anti parallel β-strands, but because there were no data on hydrogen bonds, these secondary structures could not be supported. Cyclotides are characterized by their hydrophobic properties. The formation of the cystine knot at the core of the molecule has forced the hydrophobic residues to the surface (13). The surface structure of native kalata B5 shows the hydrophobic residues (Figure 38 b and c) nicely spread out opposite to the surface structure of the misfolded kalata B5 (Figure 38 a and b). The surface structure of the misfolded peptide suggests that the structure has stabilized in this conformation because of how the hydrophobic residues have clumped together in the middle with the hydrophilic residues pointing out into the solvent.

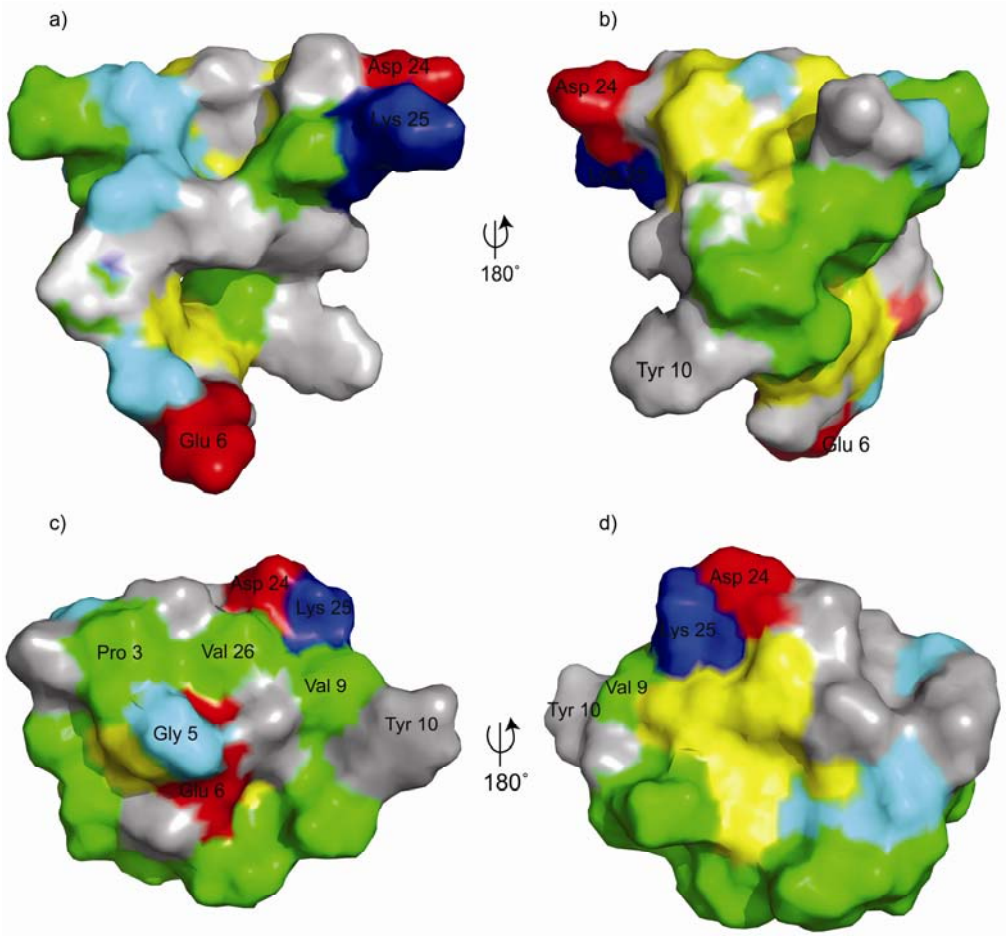

Figure 37: The surface structures of kalata B5 non-native front (a) and back (b), and kalata B5 native front (c) and back (d). The green regions are the hydrophobic residues, the blue and red regions are the charged residues, the glycines are in cyan and the cysteines are in yellow.

It has been suggested that the various biological activities of the cyclotides are due to their hydrophobic properties (13), which indicate that the non native form might not display the same activities because of a less hydrophobic surface. The glutamic acid (Glu6) is usually linking the cystine knot core to loop 3 through hydrogen bond interactions and thus helps to stabilize the cystine knot (46). The residue that is crucial for support of the cystine knot in kalata B5 non-native sticks out on the surface and hence the hydrogen bonds characteristic of the cyclotide fold is not able to be formed.

3.1.3 Insecticidal Activity of Kalata B5

Experiments from the past have shown that kalata B1 and kalata B2, both from the Möbius subfamily, possess insecticidal activity against larvae of the cotton budworm, *H. punctigera*, and the cotton bollworm, *H. armigera* (11, 48). Kalata B5 is a member of the bracelet subfamily and on the basis of previous reports that this peptide is more active as an insecticidal than the other cyclotides tested (unpublished data), it was of interest to test its activity against caterpillars. In the current study I have examined the insecticidal activity of the plant cyclotide kalata B5 isolated from *O. affinis*.

The feeding trials suggested that kalata B5 also had insecticidal activity but because of few replicates the results are not significant. Comparison of the mean numbers from a t-test shows that there is no difference between the groups. Previous feeding trials with kalata B1 have shown that it has insecticidal activity with groups of 16 replicates. Due to time constraints it was not possible to do a trial of that size. The feeding trial in this thesis attempted to give an initial idea of the activity of kalata B5 compared to kalata B1, however, with two deaths in the control group the trial suffered from very few replicates. The results did not give any significant indication that either kalata B1 or kalata B5 have insecticidal activity (t-test for all groups indicated a p-value > 50%).

The three groups of larvae in the trial differ in starting weight, with the control group having the lowest mean starting weight (2.1 mg). The groups of larvae feeding on kalata B1 and kalata B5 are more similar (2.9 mg and 3.3 mg, respectively). The optimal trial would have similar mean starting weights in the three groups. The batch of the *H. armigera* larvae might have had some issues too. Two larvae were kept outside the feeding trial and were stored in their original containers with the original diet. After 90 hours these two larvae differed in their size with the largest of them being about twice the size of the first one. This suggests that the batch was not perfect. The originally ordered batch, which the diet was made up fresh for, was cancelled due to too many deaths. Because only small amounts of kalata B5 were available, the diet was made up only once. It was then stored in the refrigerator for a week until the next batch was ready. An antifungal solution was added to the solution, but there are many other possible microorganisms or enzymes that can contribute to the breakdown of the cyclotides. That could explain the similar weight between the groups fed the diet supplemented with cyclotides and the control group. Due to time restraint this trial was made

small, but it was too small to give any significant results. The trial should be repeated again in the future with more replicates.

3.2 Conotoxins

3.2.1 Synthesis and Oxidative Folding of the κ-Conotoxin PVIIA

High selectivity for specific membrane receptors and ion channels, in addition to the fact that they are small and easily synthesized, make the conotoxins excellent drug leads. Their susceptibility to enzymatic degradation inspired the idea of cyclization, which has shown to work for some conotoxins (8). The variations between the different classes have to be taken into consideration in designing cyclic versions of them. Cyclization is potentially an effective and widely applicable approach in enhancing the suitability of disulfide-rich peptides as drugs. Optimizing the linker sizes and the folding conditions to the specific peptide will be a big step towards making conotoxins available as potential pharmacological tools, drug leads or drugs themselves.

In this study I have examined the synthesis and cyclization of the conotoxin PVIIA. It has been proven that cyclization of linear conotoxins increase their stability in human plasma (8). Clark *et al.* showed that cyclization of conotoxins with the appropriate linker give peptides with improved stability and similar biological activity to the native peptide. A linker of seven residues was shown to be the best for the α-conotoxin MII (8).

In our project we suffered from challenges with the oxidative folding. PVIIA with a thioester did cyclize, but did not fold into the native form. We believe that the peptide cyclized before the disulfide bridges were formed, which may have made it unfavorable for the peptide to make the native cysteine connectivity. When the peptide forms the cyclic backbone it will add a structural restraint that could perturb the correct folding of the peptide. A correctly sized linker is crucial in order for the cyclic peptide to be able to fold and maintain the same bioactivity while increasing the stability. Careful considerations are necessary in choosing the perfect linker to span the distance between the N and C termini. If a linker is too short it will introduce strain and disturb the folding of the synthetic peptide relative to the native structure.

This may explain the difficulties in our case with PVIIA. Linkers of four, six and seven amino acids were used in the peptide synthesis, but none of the analogues of PVIIA folded properly. They all gave poorly dispersed ^{1}H NMR spectra which suggest a lack of a well ordered three dimensional structure. The seven-residue-linker that worked well with the α-conotoxin MII (8) did not work out well for our κ-conotoxin. The conserved features of the α-conotoxins (i.e. α-helix and the I-III and II-IV disulfide connectivity) do not apply for PVIIA, which is a κ-conotoxin. The lengths of the two peptides differ as well. The MII is a 16 residue peptide with two disulfides, whereas PVIIA consist of 27 residues and has three disulfides. With 11 more amino acids in its chain, PVIIA is a more complex conotoxin and therefore may require further considerations in predicting linker lengths.

PVIIA was finally synthesized without the thioester in attempt to make the disulfide bridges form before the cyclization. The linear peptide was oxidized and isolated, and ^{1}H NMR experiments showed a well dispersed spectrum which confirmed the folding of the peptide. This shows that it was not the additional residues to the termini in the earlier trials that caused a misfolding but the cyclization itself.

Three different methods were attempted to make the folded peptide cyclic; HBTU and DIPEA in DMF (i), PyBOP and DIPEA in DCM (ii) and HOBt and EDC in DMSO (iii). With the first method the peptide either vanished or it was in such low concentration that it could not be isolated in sufficient amounts on the RP-HPLC to be recognized on the ES-MS. This problem has been reported previously for HBTU and DIPEA couplings (49).

The second method with PyBOP and DIPEA in DCM made a polymeric byproduct. The linear peptide was also observed in some of the fractions, which shows that some of the peptide did not react at all. The polymer was first observed in iib) when the peptide concentration was 0.2 mg/ml. The peptide concentration was reduced in an attempt to force the peptide to react with itself. In the two following reactions with method ii) the peptide concentrations were reduced to 0.07 mg/ml and 0.01 mg/ml in method c and d, respectively. The polymeric byproduct still appeared and there were no masses of the cyclic PVIIA observed on the ES-MS. PyBOP and DIPEA are strong reaction agents and reactions between all carboxyl- and amide groups can easily proceed. PVIIA contain several amino acids with carboxyl- and amide groups. Arginine, lysine, and histidine contain an amide in their side chains whereas aspartic acid contains carboxyl groups in their side chains. Reactions between

these might have happened as well as dimerization between multiple peptides. I was not able to identify the masses from the reaction with method iii). Due to time constraints, there was no time to modify these reactions further, a procedure that would have been followed if there was enough time.

The last method with HOBt and EDC in DMSO did show some very small amounts of the masses of a cyclic PVIIA, but it was too little to be reliable. Some of the peptide had not reacted at all as the linear peptide was identified on the ES-MS. Method iii) also produced some byproducts, which we were not able to identify as anything related to PVIIA. The experiments were repeated with less concentrated peptide in attempt to favor formation of a cyclic monomer rather than intermolecular dimer formation, but the results showed the same as in the method with higher peptide concentrations.

4 Conclusion

In my project I have synthesized and examined the activity of kalata B5. The synthesis of the bracelet cyclotide kalata B5 resulted in a misfolded product. The structure determination of the misfolded product indicated a very flexible region between residues 1-11. We were not able to determine the disulfide connectivity using reduction-alkylation. Since kB5nn and CVO2nn (another misfolded bracelet cyclotide) showed similar Hα chemical shifts and Hα secondary shifts, the disulfide connectivity of CVO2nn was used for kB5nn (I-II, III-IV, V-VI). Peptides of the bracelet subfamily are known to be difficult to fold. The study of the structure of the misfolded kalata B5 should be investigated further in attempt to find answers of why the misfolding happened. Information about factors that can cause misfolding is essential for successful synthesis of bracelet cyclotides in the future. The fact that this is the main subfamily makes this kind of knowledge even more important as these peptides have great potential in the commercial pharmaceutical world.

Isolated kalata B5 was investigated for its insecticidal activity against the larvae *H. armigera*, but owing to small groups and a short trial, the larvae trial did not give any significant results. However, the larvae assay suggested that kalata B5 has insecticidal activity, but not more than kalata B1. A larger trial is necessary to give significant results about the insecticidal activity of kalata B5.

In the study of cyclization of the conotoxin PVIIA there were also challenges regarding the proper folding of the peptide. PVIIA was synthesized with different linkers, different protecting groups on the cysteines, and both with and without a thioester. A total of 33 oxidation conditions were examined for the peptides. It was not until the peptide was synthesized without the thioester that it folded into its native conformation, which means it was linear while it folded. Similar Hα chemical shifts and Hα secondary shifts between synthesized PVIIAs7 and the native PVIIA confirmed the native folding of the synthesized peptide. Three different reaction agents were investigated for the cyclization of the oxidized PVIIAs7, but none of them resulted in a cyclic PVIIA. Method ii) might have produced small amounts of the cyclic PVIIA7, but the identification of the masses of a cyclic peptide could not be trusted as the intensity of the ES-MS analyses were too low to give a significant result.

PVIIA is a 27 amino acid long tightly folded peptide. To be able to cyclize the peptide, close considerations regarding linker size are crucial. In the very last part of my thesis I was close to producing a cyclic version of the PVIIA, but due to time constraints I was not able to optimize the cyclization conditions further (both method ii and iii). Promising progress has been achieved towards the synthesis of a cyclic PVIIA analogue and the project is one step away from discovering the optimized conditions for cyclization. This will be a big step towards a potential new drug or drug lead from the conotoxins.

5 Materials and Methods

5.1 Kalata B5

5.1.1 Synthesis of Kalata B5

Kalata B5 was synthesized on a PAM-Gly resin (0.50 mmol scale, 1.06 g) by SPPS using *in situ* neutralization/HBTU (2-(1H-Benzotriazole-1-yl)-1,1,3,3-tetramethyluronium hexafluorophosphate) protocol for Boc chemistry (42). Because kalata B5 is a cyclic peptide, thioester-based cyclization is required and the synthesis has to end with a cysteine residue at the N-terminus. The peptide was therefore synthesized from Gly19 and finished with Cys20. After the peptide was synthesized it was cleaved with HF, purified with RP-HPLC with 1 % gradient buffer B in A at a flow rate of 8 ml/min.

5.1.2 Oxidative Folding and Cyclization of Kalata B5

Several folding conditions were examined for the linear kalata B5 (Table 1, Appendix 1, condition: 3, 9, 10, 18, 21, 22, 24-26, 28, 31-34). By analyzing them on the analytical reversed phase high performance liquid chromatography (RP-HPLC) condition 18 was found to give the best yield. Approximately 10 mg of the fully reduced peptide was oxidized in 50:50 0.1 M NH_4HCO_3 and propan-2-ol at 4˚C for 24 hours. After identification of the correct mass on the electrospray mass spectrometry (ES-MS) the oxidized peptide was analyzed by 1D ^1H NMR on a Bruker 600-MHz spectrometer and RP-HPLC for comparison with the natural kalata B5 (isolated from *O. affinis*).

5.1.3 Determination of the Disulfide Connectivity in Kalata B5 Non-Native

The close packing of the six cysteine residues makes determination of the disulfide connectivity by NMR difficult (50). The disulfide connectivity in kalata B5 non-native was

tried solved by partial reduction (with 20 mM TCEP in citrate buffer, pH 3) and selective labeling via alkylation (with 60 mM NEM). This method was also used to determine the disulfide connectivity in kalata B1 and confirmed the presence of the cystine knot in the prototypic cyclotide (50).

Peptides (~ 0.5 mg in 0.5 ml of buffer A and ~ 30% buffer B as eluted from HPLC) were incubated with an equivalent volume of 20 mM TCEP and 0.2 M citrate buffer, pH 3.0, at 37˚C for 4 minutes. By immediate injection on a Phenomenex Jupiter C18 column (250x4.6 (inner diameter) mm, 5μm, 300 Å), the reaction was stopped. The peptide eluted with a shallow gradient at a flow rate of 1 ml/min (isocratic at 20% B for 10 min; 20-34% B in 3 min; 34-40% B in 24 min; 40-100% B for 1 min, 100% for 2 min; and finally re-equilibration at 20% B for 11 min, giving a total time of 51 min). Partially reduced species were collected manually. To the fractions containing the peaks of interest were an equal volume of 60 mM N-ethyl-maleimide (NEM) in 0.2 M citrate buffer (pH 3) added. This method was pursued with incubation time both at room temperature for 15 hours and 37˚C for 2 hours. The reaction mixture was then loaded onto the HPLC and peaks collected and analyzed by ES-MS.

5.1.4 Feeding Trials with Kalata B5

The artificial diet was made up by wheat germ (6.55 %), yeast (5.46 %), soy flour (7.42 %), nipagin (0.33 %), sorbic acid (0.11 %) and l-ascorbic acid (0.33 %) in three plastic containers, A, B and C. Kalata B1 (0.5 μmol) and kalata B5 (0.5 μmol) were added to diet A and B, respectively, while diet C was kept as a negative control. This was heated and added anti-fungal solution (0.11 %) and 546 μL agar solution (27.3 %, made of 83.2 mg agar in 2 ml hot tap water which was heated at 60˚C). Holes were pierced in the lids of 12 eppendorf tubes and 12 plastic containers with a syringe needle to provide aeration and lining tissues were put under the lids to prevent escape of larvae. The feeding containers were prepared by weighing in 250 mg diet. Cotton bollworms (*H. armigera*) were received from QDPI (Queensland Department of Primary Industries, Indooroopilly, QLD 4068, Australia). After 6 hours of starvation the larvae where transferred into appropriately labeled feeding containers. A wet towel was put on the top of the feeding containers to maintain humidity and prevent diet from

dehydration. After 18, 42, 66, and 90 hours of feeding the larvae were observed and weighed. For each weighing the larvae were transferred to the eppendorf tubes. On the last day the weight of the frass and the remaining diet were also measured. This day the larvae were photographed individually and comparatively.

The cyclotides kalata B1 and kalata B5, which were used in the feeding trials of the *H. armigera,* were provided by Dr Josh Mylne and Crystal Huang. Both the cyclotides have been isolated from the plant *O. affinis* using standard methods.

5.2 PVIIA

5.2.1 Design and synthesis of Three Analogues of the κ-Conotoxin PVIIA with both Acm- and MeBzl Protecting Groups

The κ-conotoxin PVIIA was synthesized with three different linkers; TRNG, GGAAGG, GGAAGAG. These linkers were designed by Dr Richard Clark and based on analyses of homology models generated by using the structural coordinate file of PVIIA (Protein Data Bank ID 1AV3 PVIIA, available from the PDB; www.rcsb.org/pdb) and the MODELER module within INSIGHT II (Accelrys, Inc., San Diego).

The three analogues were synthesized manually by SPPS using Boc chemistry, starting from a PAM-Gly resin (0.5 mmol scale, 1.06 g resin), and amino acids were added to the resin using HBTU with *in situ* neutralization (42). Acm protected cysteines were used for CIII and CVI. Since the peptides synthesized are cyclic the NCL strategy was used (43).

The couplings were determined using the ninhydrin test (51). A yield higher than 99.6% was used to move on the next amino acid. Another approach was to look at the color where the absence of the blue color was an indication that the reaction of the resin-bound amino groups was complete. The peptide was cleaved from the resin using HF with p-cresol and thiocresol as scavengers (HF:*p*-cresol:*p*-thiocresol; 18:1:1 *v*/*v*/*v*) at -5-0˚C for 1.5 hour. After cleavage, the peptides were precipitated with diethyl ether, filtered and redissolved in 50% acetonitrile, 0.1% TFA and lyophilized.

The crude peptides were purified by RP-HPLC using a 1% gradient (100% solvent A to 80% solvent B in 80 minutes). Buffer A consists of 0.1% TFA in H_2O while buffer B is 0.045% TFA, 10% H_2O, 90% CH_3CN. The purity and molecular weight of the peptides were confirmed by ES-MS.

5.2.2 Folding and Cyclization of the Three Analogues; PVIIA-GNRT, PVIIA-GGAAGG, PVIIA-GGAAGAG

Up-scaled cyclization and partial oxidation of the reduced linear peptide were carried out in a buffered solution of 0.1 M NH_4HCO_3 containing the appropriate concentration of the peptide (10 mg in 50 ml buffer solution). The reaction was kept at 4˚C on a magnetic stirrer overnight and purified the next day.

The iodine oxidation of the Acm protecting cysteines was achieved by dissolving the partially oxidized, partially protected cyclic peptide in 50 % acetic acid and have nitrogen bubbled through the solution for 5 min. 1 M HCl was then added followed immediately by adding 0.1M I_2 in 50 % aqueous acetic acid until solution was yellow. The flask was then flushed with nitrogen, wrapped in aluminum foil and left for 20 hours. The reaction was quenched with a spatula tip size of solid ascorbic acid, and the solution turned colorless. The solution was then diluted with buffer A before isolating the peptide by RP-HPLC as described above. Following purification and isolation on RP-HPLC the peptide was analyzed by ^1H NMR on a Bruker 600-MHz spectrometer to check the folding of the peptide.

5.2.3 Synthesis and Oxidative Folding of PVIIA7 with only MeBzl Protecting Groups

PVIIA-GGAAGAG (referred as PVIIA7) was synthesized with only MeBzl protected cysteine. *In situ* Boc chemistry was used with a PAM-Gly resin (0.5 mmol scale, 1.06 g resin). The peptide was cleaved with HF and purified by RP-HPLC followed by oxidation with 0.1 M NH_4HCO_3 (10 mg peptide in 50 ml buffer) and stirred at 4˚C overnight. After purification and isolation by RP-HPLC the folding of the peptide was analyzed on the by 1D ^1H NMR on a Bruker 600-MHz spectrometer to check the folding of the peptide.

5.2.4 Synthesis of PVIIA without the Thioester Linker

PVIIA, with GAGG added on the N terminus and GAG added on the C terminus, was synthesized without the thioester linker. This peptide is thru the rest of the theses referred as PVIIAs7 when it is linear, which means its seven residue linker is split, and cPVIIA7 when it is referred to the cyclic form. With the achiral glycines reacting in the cyclization process only one isomer is produced. The synthesis was conducted with Microwave-assisted (Liberty CEM Microwave Peptide Synthesizer with PepDriver software) Fmoc SPPS using 2-chloro-trityl resin (0.25 mmol scale, 0.19 g resin). The resin was cleaved with TFA and the peptide was purified and identified by RP-HPLC and ES-MS.

5.2.5 Folding of PVIIAs7 without the Thioester Linker

Approximately 10 mg of pure PVIIAs7 was oxidized with 0.1 M NH_4OAc pH 7.9, 1 mM GSH and 0.1 mM GSSG (peptide concentration 0.2 mg/ml) at 4˚C for 24 hours, and the folding was confirmed by 1D ^1H NMR on a Bruker 500-MHz spectrometer to check the folding of the peptide.

5.2.6 Cyclization Trials of the PVIIA7s7 without the Thioester Linker

Approximately 100 µg of peptide was dissolved in 183 µL DMF and 16 µL DIPEA and 1 µL 0.5M HBTU were added. The reaction was stopped after 1 minute with 10 µL TFA and separated on a 1 ml/min column and 2% gradient. The masses of the peaks were analyzed on the ES-MS.

5.3 Analytical Instruments used in the Purification and Identification of the Peptides

5.3.1.Analytical HPLC

Analytical HPLC was either performed on a Waters 600 Controller system equipped with a Waters 2487 Dual λ Absorbance Detector and Empower software or an Agilent 1100 Series with ChemStation software. On the Waters 600 the samples were auto-injected using Waters 717plus. The column used for analyzing the purity was a Phenomenex Jupiter C18 analytical column (150x2.00mm 5 micron, 300 Å pore size, 5µm particle size). Samples were eluted at a flow rate of 0.3 ml/min with a linear gradient of 0-80 % (buffer B in buffer A) for 40 minutes with UV detection at 215 nm. The column used for the disulfide connectivity determination of kalata B5 was a Phenomenex C18 column (250 x 4.60 mm 5 micron, 300 Å pore size, 5µm particle size) with a flow rate of 1 ml/min.

5.3.2 Semipreparative HPLC

Semipreparative HPLC was performed on a Waters 600-ES-MS System Controller system equipped with either a Waters 484 Tunable Absorbance Detector or a Waters 2487 Dual λ Absorbance Detector. Samples were manually loaded onto a Phenomenex Jupiter C18 column (250x10.00 5 micron, 300 Å pore size, 5 µm particle size) and eluted at a flow rate of 3 ml/min with a linear gradient of 0-80 % Buffer B for 80 minutes with UV detection at 215 nm.

5.3.3 Preparative HPLC

All preparative HPLC was performed on a Waters 600-ES-MS System Controller system equipped with either a Waters 484 Tunable Absorbance Detector or a Waters 2487 Dual λ Absorbance Detector. Samples were manually loaded onto a Phenomenex Jupiter C18 column (250x21.20mm, 300 Å pore size, 15 µm particle size) and eluted at a flow rate of 8 ml/min with a linear gradient of 0-80 % Buffer B for 80 minutes with UV detection at 215 nm.

5.3.4 Mass Spectrometry

The identification of HPLC peak constituents was based on mass and all mass data was obtained using electrospray/time of flight mass spectroscopy on a Micromass ZMD instrument with a Perkin Elmer series 200 lc pump absorbance detector and MassLynx version 3.5 software.

5.3.5 NMR-Experiments

NMR data for PVIIA and the cyclotide kalata B5 non-native were all derived using NMR spectroscopy. The peptides were dissolved in 90% H_2O (500µL Milli-Q water) and 10% D_2O (50 µL). 2D NMR experiments included DQF-COSY, E-COSY, TOCSY and NOESY spectra and were acquired on a Bruker 500- MHz spectrometer or a Bruker 600-MHz spectrometer. The spectra were acquired at 298 K. TOCSY and NOESY spectra were acquired with 150 and 300 ms mixing times. Information on slowly exchanging amide protons was obtained by acquisition of 1-D and TOCSY spectra immediately upon dissolution of a fully protonated peptide in D_2O. All spectra were analyzed on Silicon Graphics Indigo workstations using TOPSPIN (Bruker) and Sparky software. Spectra were assigned using the sequential assignment technique (45).

5.3.6 Structure Calculations

NOE restraints were obtained from the peak heights in 150- and 300-ES-MS NOESY spectra. Backbone dihedral angle restraints were derived from $^3J_{HN\text{-}H\alpha}$ coupling constants measured from either 1D ^{1}H NMR spectra or from a 2D DQF-COSY spectrum. Appropriate pseudo-atom corrections were applied. Angles were restrained to -60°±30° for $^3J_{HN\text{-}H\alpha}$ <5 Hz and -120°±30° for $^3J_{HN\text{-}H\alpha}$ > 8.5 Hz. Additional φ angle restraints of -100°±80° were applied in cases where the intra residue dαN(i,i) NOE was clearly weaker than then sequential dαN(i,i+1) NOE. Intraresidue NOE and $^3J_{H\alpha\text{-}H\beta}$ coupling patterns, determined from an E-COSY spectrum, were used in assigning the χ^1 angle conformations of side chains. Initial structures were generated by using CYANA software (52). Fifty structures were calculated

and the final 20 structures with the lowest overall energies which had no violations of NOE restraints > 0.15 Å or dihedral angle restraints>2.0˚ were retained for analysis. Structures were visualized with the program MOLMOL (53) and analyzed with PROMOTIF (54) and PROCHECK_NMR (55).

6 References

1. Trabi M & Craik DJ (2002) Circular proteins - no end in sight. *Biochemical Sciences* 27(3):132-138.
2. Saether O*, et al.* (1995) ELUCIDATION OF THE PRIMARY AND 3-DIMENSIONAL STRUCTURE OF THE UTEROTONIC POLYPEPTIDE KALATA B1. *Biochemistry* 34(13):4147-4158.
3. Martinezbueno M*, et al.* (1994) DETERMINATION OF THE GENE SEQUENCE AND THE MOLECULAR-STRUCTURE OF THE ENTEROCOCCAL PEPTIDE ANTIBIOTIC AS-48. *Journal of Bacteriology* 176(20):6334-6339.
4. Tang Y-Q*, et al.* (1999) A Cyclic Antimicrobial Peptide Produced in Primate Leukocytes by the Ligation of Two Truncated -Defensins. *Science* 286(5439):498-502.
5. Luckett S*, et al.* (1999) High-resolution structure of a potent, cyclic proteinase inhibitor from sunflower seeds. *Journal of Molecular Biology* 290(2):525-533.
6. Bulaj G (2005) Formation of disulfide bonds in proteins and peptides. *Biotechnology Advances* 23:87-92.
7. Daly NL, Love S, Alewood PF, & Craik DJ (1999) Chemical Synthesis and Folding Pathways of Large Cyclic Polypeptides: Studies of the Cystine Knot Polypeptide Kalata B1. *Biochemistry* 38(32):10606-10614.
8. Clark RJ*, et al.* (2005) Engineering stable peptide toxins by means of backbone cyclization: Stabilization of the alfa-conotoxin MII. *PNAS* 102(39):13767-13772.
9. Lovelace ES*, et al.* (2006) Cyclic MrIA: A Stable and Potent Cyclic Conotoxin with a Novel Topological Fold that Targets the Norepinephrine Transporter. *Journal of Medicinal Chemistry* 49(22):6561-6568.
10. Gran L (1973) EFFECT OF A POLYPEPTIDE ISOLATED FROM KALATA-KALATA (OLDENLANDIA-AFFINIS DC) ON ESTROGEN DOMINATED UTERUS. (Translated from English) *Acta Pharmacologica Et Toxicologica* 33(5-6):400-408 (in English).
11. Jennings C, West J, Waine C, Craik DJ, & Anderson M (2001) Biosynthesis and insecticidal properties of plant cyclotides: The cyclic knotted proteins form *Oldenlandia affinis*. *PNAS* 98(19):10614-10619.

12. Craik DJ, Daly NL, Bond T, & Waine C (1999) Plant Cyclotides: A uniqe family of cyclic and knotted proteins that defines the cyclic cystine knot structural motif. *Journal of Molecular Biology* 294:1327-1336.
13. Craik DJ, Daly NL, Mulvenna J, Plan MR, & Trabi M (2004) Discovery, structure and biological activities of the cyclotides. *Current Protein & Peptide Science* 5(5):297-315.
14. Plan MRR*, et al.* (2007) The Cyclotide Fingerprint in *Oldenlandia affinis*: Elucidation of Chemically Modified, Linear and Novel Macrocyclic Peptides. *ChemBioChem* 8:1001-1011.
15. Craik DJ, Simonsen S, & Daly NL (2002) The cyclotides: Novel macrocyclic peptides as scaffolds in drug design. *Current Opinion in Drug Discovery & Development* 5(2):251-260.
16. Felizmenio-Quimio ME, Daly NL, & Craik DJ (2001) Circular proteins in plants - Solution structure of a novel macrocyclic trypsin inhibitor from Momordica cochinchinensis. *Journal of Biological Chemistry* 276(25):22875-22882.
17. Daly NL, Clark RJ, Plan MR, & Craik DJ (2006) Kalata B8, a novel antiviral circular protein, exhibits conformational flexibility in the cystine knot motif. *Biochemical Journal* 393:619-626.
18. Tam JP, Lu Y-A, Yang J-L, & Chiu K-W (1999) An unusual structural motif of antimicrobial peptides containing end-to-end macrocycle and cystine-knot disulfides. *PNAS* 96:8913-8918.
19. Schöpke T, Hasan Agha MI, Kraft R, Otto A, & Hiller K (1993) Hämolytisch aktive Komponenten aus *Viola tricolor* L. and *Viola arvensis* Murray. *Scientia Pharmaceutica* 61:145-153.
20. Gustafson KR, McKee TC, & Bokesch HR (2004) Anti-HIV cyclotides. *Current Protein & Peptide Science* 5(5):331-340.
21. Witherup KM*, et al.* (1994) CYCLOPSYCHOTRIDE-A, A BIOLOGICALLY-ACTIVE, 31-RESIDUE CYCLIC PEPTIDE ISOLATED FROM PSYCHOTRIA-LONGIPES. *Journal of Natural Products-Lloydia* 57(12):1619-1625.
22. Goransson U, Sjogren M, Svangard E, Claeson P, & Bohlin L (2004) Reversible antifouling effect of the cyclotide cycloviolacin O2 against barnacles. *Journal of Natural Products* 67(8):1287-1290.

23. Lindholm P*, et al.* (2002) Cyclotides: A novel type of cytotoxic agents. *Molecular Cancer Therapeutics* 1(6):365-369.
24. Government Q (2009) Insect management in cotton.
25. CRC CCC (2007) Australian Cotton Comparative Analysis 2006.
26. Terlau H & Olivera BM (2004) Conus Venoms: A rich source of Novel Ion Channel-Targeted Peptides. *Physiol. Rev.* 84:41-68.
27. Terlau H*, et al.* (1996) Strategy for rapid immobilization of prey by a fish-hunting marine snail. *Letters to Nature* 381:148-151.
28. Lewis RJ & Garcia ML (2003) Therapetutic potential of venom peptides. *Nature Reviews* 2(doi:10.1038/nrd1197):790-802.
29. Adams DJ, Alewood PF, Craik DJ, Drinkwater RD, & Lewis RJ (1999) Conotoxins and Their Potential Pharmaceutical Applications. *Drug Developement Research* 46:219-234.
30. A. Grey Craig PB, Baldomero M. Olivera, (1999) Post-translationally modified neuropeptides from Conus venoms. *European Journal of Biochemistry* 264(2):271-275.
31. Craik DJ & Adams DJ (2007) Chemical Modification of Conotoxins to Improve Stability and Activity. *ACS Chemical Biology* 2(7):457-468.
32. Livett BG*, et al.* (2006) Therapeutic applications of conotoxins that target the neuronal nicotinic acetylcholine receptor. *Toxicon*:1-20.
33. Scanlon M*, et al.* (1997) Solution structure and proposed binding mechanism of a novel potassium channel toxin κ-conotoxin PVIIA. *Structure* 5(12):1585-1597.
34. Millard EL, Daly NL, & Craik DJ (2004) Structure-activity relationships of alpha-conotoxins targeting neuronal nicotinic acetylcholine receptors. *European Journal of Biochemistry* 271:2320-2326.
35. Clark RJ, Fischer H, Nevin ST, Adams DJ, & Craik DJ (2006) The Synthesis, Structural Characterization, and Receptor Specificity og the alpha-Conotoxin Vc1.1*. *Journal of Biological Chemistry* 281(32):23254-23263.
36. Prommer E (2006) Ziconotide: A new option for refractory pain. *Drugs of Today* 42(6):369-378.
37. Bowersox SS & Luther R (1998) Pharmacotherapeutic potential of omega-conotoxin MVIIA (SNX-111), an N-type neuronal calcium channel blocker found in the venom of Conus magus. *Toxicon* 36(11):1651-1658.

38. Deechongkit S & Kelly JW (2002) The Effect of Backbone Cyclization on the Thermodynamics of β-Sheet Unfolding: Stability Optimization of the PIN WW Domain. *Journal of the American Chemical Society* 124:4980-4986.
39. Hubbard SJ (1998) The structural aspects of limited proteolysis of native proteins. *Biochimica et Biophysica Acta (BBA) - Protein Structure and Molecular Enzymology* 1382(2):191-206.
40. Shon K-J*, et al.* (1998) k-Conotoxin PVIIA Is a Peptide Inhibiting the Shaker K^+ Channel. *The Journal of Biological Chemistry* 273(1):33-38.
41. Merrifield RB (1963) Solid Phase Peptide Synthesis. I. The Synthesis of a Tetrapeptide. *Journal of the American Chemical Society* 85(14):2149-2154.
42. Schnölzer M, Alewood PF, Jones A, Alewood D, & Kent SBH (2007) *In Situ* Neutralization in Boc-chemistry Solid Phase Peptide Synthesis. *International Journal of Peptide Research and Therapeutics* 13:31-44.
43. Dawson PE, Muir TW, Clark-Lewis I, & Kent SBH (1994) Synthesis of Proteins by Native Chemical Ligation. *Science* 266(5186):776-779.
44. Cemazar M, Joshi A, Daly NL, Mark AE, & Craik DJ (2008) The Structure of a Two-Disulfide Intermediate Assists in Elucidating the Oxidative Folding Pathway of a Cyclic Cystine Knot Protein. *Structure* 16:842-851.
45. Wüthrich K (1986) *NMR of proteins and nucleic acids* (A Wiley-Interscience Publication, John Wiley & Sons, New York).
46. Rosengren KJ, Daly NL, Plan MR, Waine C, & Craik DJ (2003) Twists, knots, and rings in proteins - Structural definition of the cyclotide framework. *Journal of Biological Chemistry* 278(10):8606-8616.
47. DeLa Cruz R, Whitby FG, Buczek O, & Bulaj G (2003) Detergent-assisted oxidative folding of delta-conotoxins. *Journal of Peptide Research* 61(4):202-212.
48. Jennings C*, et al.* (2005) Isolation, Solution Structure, and Insecticidal Activity of Kalata B2, a Cirular Protein with a Twist: Do Möbius Strips Exist in Nature? *Biochemistry* 44:851-860.
49. Trabi M, Schirra HJ, & Craik DJ (2001) Three-Dimensional Structure of RTD-1, a Cyclic Antimicrobial Defensin from Rhesus Macaque Leukocytes. *Biochemistry* 40:4211-4221.
50. Göransson U & Craik DJ (2003) Disulfide Mapping of the Cyclotide Kalata B1. *The Journal of Biological Chemistry* 278(48):48188-48196.

51. Sarin VK, Kent SBH, Tam JP, & Merrifield RB (1981) Quantitative Monitoring of Solid-Phase Peptide Synthesis by the Ninhydrin Reaction. *Analytical Biochemistry* 117:147-157.

52. Ikeya T, Terauchi T, Guntert P, & Kainosho M (2006) Evaluation of stereo-array isotope labeling (SAIL) patterns for automated structural analysis of proteins with CYANA. *Magnetic Resonance in Chemistry* 44:S152-S157.

53. Koradi R, Billeter M, & Wuthrich K (1996) MOLMOL: A program for display and analysis of macromolecular structures. *Journal of Molecular Graphics* 14(1):51-&.

54. Hutchinson EG & Thornton JM (1996) PROMOTIF - A program to identify and analyze structural motifs in proteins. (Translated from English) *Protein Sci.* 5(2):212-220 (in English).

55. Laskowski RA, Macarthur MW, Moss DS, & Thornton JM (1993) PROCHECK - A PROGRAM TO CHECK THE STEREOCHEMICAL QUALITY OF PROTEIN STRUCTURES. *Journal of Applied Crystallography* 26:283-291.

7 Appendix

Appendix 1
Oxidation conditions 1-22

	Buffer	Temperature (°C)	Time (hr)	Peptide conc. (mg/mL)
1	50 mM NH_4OAc, 2M$(NH_4)_2SO_4$, 1mM EDTA, 1mM GSH, 0.1 mM GSH, 0.1 mM GSSG, pH 7.7	4	24	0.5
2	50 mM NH_4OAc, 2M$(NH_4)_2SO_4$, 1mM EDTA, 1mM GSH, 0.1 mM GSH, 0.1 mM GSSG, pH 7.7	22	24	0.5
3	0.1 M NH_4HCO_3, pH 8.2	4	24	0.5
4	0.1 M NH_4HCO_3, pH 8.2	22	24	0.5
5	0.1 M NH_4HCO_3, 1 mM GSH, 0.1 mM GSSG	4	24	0.5
6	0.1 M NH_4HCO_3, 1 mM GSH, 0.1 mM GSSG	22	24	0.5
7	0.1% TFA (buffer A used), 1 mM GSH, 0.5 mM GSSG. 5µM peptide (0.5 mL)	4	24	0.2
8	0.1% TFA (buffer A used), 1 mM GSH, 0.5 mM GSSG. 5µM peptide (0.5 mL)	22	24	0.2
9	0.1 M NH_4HCO_3, 2 mM GSH, 0.4 mM GSSG	4	24	0.5
10	0.1 M NH_4HCO_3, 2 mM GSH, 0.4 mM GSSG	22	24	0.5
11	0.1 M NH_4HCO_3, 5 mM GSH, 0.5 mM GSSG	4	24	0.5
12	0.1 M NH_4HCO_3, 5 mM GSH, 0.5 mM GSSG	22	24	0.5
13	0.1 M NH_4HCO_3, 15% methanol, pH 7.9	4	24	0.5
14	0.1 M NH_4HCO_3, 15% methanol, pH 7.9	22	24	0.5
15	0.126 M NH_4HCO_3, 2.5mM GSH, 0.25mM GSSG, 0.5M GnHCl, 25% methanol	4	24	0.5
16	0.126 M NH_4HCO_3, 2.5mM GSH, 0.25mM GSSG, 0.5M GnHCl, 25% methanol	22	24	0.5
17	0.126 M NH_4HCO_3, 2.5mM GSH, 0.25mM GSSG, 0.5M GnHCl, 50% methanol	22	24	0.5
18	50:50 0.1 M NH_4HCO_3 and propan-2-ol	4	24	0.5
19	50:50 0.1 M NH_4HCO_3 and propan-2-ol, 1mM GSH	4	24	0.5
20	50:50 0.1 M NH_4HCO_3 and propan-2-ol, 1mM GSH	22	24	0.5
21	50:50 0.1 M NH_4HCO_3 and propan-2-ol, 2 mM GSH, 0.4 mM GSSG	4	24	0.5
22	35% DMSO, 0.1 M Tris-HCl (pH 8.5), 1 mM EDTA, 2 mM GSH, 2 mM cystamine, 6% Brij35	4	24	0.5

Appendix 1
Conditions 23-44

	Buffer	Temperature (˚C)	Time (hr)	Peptide conc. (mg/mL)
23	35% DMSO, 0.1 M Tris-HCl (pH 8.5), 1 mM EDTA, 2 mM GSH, 2 mM cystamine, 6% Brij35	22	24	0.5
24	2 M $(NH_4)_2SO_4$	4	24	0.5
25	2 M $(NH_4)_2SO_4$, 5mM GSH, 1mM GSSG	4	24	0.5
26	0.1 M NH_4OAc	4	24	0.5
27	0.1 M NH_4OAc	22	24	0.5
28	0.1 M NH_4OAc, 5mM GSH, 1mM GSSG	4	24	0.5
29	0.1 M NH_4OAc, 1mM GSH, 0.1mM GSSG, pH 7.9	4	24	0.5
30	0.1 M NH_4OAc, 1mM GSH, 0.1mM GSSG, pH 7.9	22	24	0.5
31	Na_3PO_4	4	24	0.5
32	Na_3PO_4, 5mM GSH, 1mM GSSG	4	24	0.5
33	0.33 M NH_4OAc, 0.5 GnHCl	4	24	0.5
34	0.33 M NH_4OAc, 0.5 GnHCl, 5mM GSH, 1mM GSSG	4	24	0.5
35	0.1 M MOPS, pH 7.5	4	24	0.5
36	0.1 M MOPS, pH 7.5	22	24	0.5
37	0.1 M MOPS, 30% isopropanol, pH 7.5	4	24	0.5
38	0.1 M MOPS, 30% isopropanol, pH 7.5	22	24	0.5
39	2 M GnHCl, 5mM GSH, 0.5mM GSSG, 50mM NH_4OAc, pH 7.4	4	24	0.5
40	2 M GnHCl, 5mM GSH, 0.5mM GSSG, 50mM NH_4OAc, pH 7.4	22	24	0.5
41	0.1 M Tris, 5mM GSH, 0.5mM GSSG, 2 M urea, pH 8.5	4	24	0.5
42	0.1 M Tris, 5mM GSH, 0.5mM GSSG, 2 M urea, pH 8.5	22	24	0.5
43	0.1 M Tris-HCl, 1mM EDTA, 2mM GSH, 1mM GSSG	4	24	0.5
44	0.1 M Tris-HCl, 1mM EDTA, 2mM GSH, 1mM GSSG	22	24	0.5